frontiers | Frontiers in Earth Science

TYPE Original Research
PUBLISHED 16 March 2023
DOI 10.3389/feart.2023.1136397

Check for updates

OPEN ACCESS

EDITED BY
Huan Li,
Central South University, China

REVIEWED BY
Liang Qiu,
China University of Geosciences, China
Mohammad Yazdi,
Shahid Beheshti University, Iran

*CORRESPONDENCE
Han Runsheng,
554670042@qq.com
Zhang Yan,
78598874@qq.com

SPECIALTY SECTION
This article was submitted to Geochemistry, a section of the journal Frontiers in Earth Science

RECEIVED 03 January 2023
ACCEPTED 28 February 2023
PUBLISHED 16 March 2023

CITATION
Runsheng H, Yan Z, Wenlong Q, Tianzhu D, Mingzhi W and Feng W (2023), Geology and geochemistry of Zn-Pb(-Ge-Ag) deposits in the Sichuan-Yunnan-Guizhou Triangle area, China: A review and a new type.
Front. Earth Sci. 11:1136397.
doi: 10.3389/feart.2023.1136397

Geology and geochemistry of Zn-Pb(-Ge-Ag) deposits in the Sichuan-Yunnan-Guizhou Triangle area, China: A review and a new type

Han Runsheng[1]*, Zhang Yan[1]*, Qiu Wenlong[1], Ding Tianzhu[2], Wang Mingzhi[1] and Wang Feng[3]

[1]Kunming University of Science and Technology, Southwest of Geological Survey, Geological Survey Center for Non-ferrous Mineral Resources, Kunming, China, [2]Sichuan Huidong Daliang Mining Co., Ltd., Huidong, China, [3]Yunnan Metallurgy Resources Exploration Co., Ltd., Kunming, China

Mississippi Valley Type (MVT)[1] deposits represent the majority of carbonate-hosted Zn–Pb deposits globally. They typically form in an extensional tectonic setting along passive margins. However, studies on carbonate-hosted Zn–Pb deposits in the Sichuan–Yunnan–Guizhou Triangle area (SYGT) reveal differences in terms of the essential features of typical MVT deposits. We discuss the main features of these deposits, controlled by folds and faults, high-grade Zn–Pb ores and symbiotic or associated elements (i.e., abundant Ag and dispersed amounts of Ge, Ga, and Cd) of significant economic value. Based on a comparison of Pb-Zn deposits in SYGT and classical MVT deposits formed in an extensional tectonic setting, as well as a subsequent discussion on deposit classification, we propose that the Huize-style Zn–Pb deposits are a new deposit style, whose basic features can guide future ore exploration. We define the Huize-style deposits based on four factors: i) Hierarchical ore-controlling system of strike-slip fault-fold structures, ii) litho-facies associated with typical alternation and mineralisation, iii) ore-forming geochemical features revealed by typical mineral assemblages, mineralisation alteration zoning, fluid-inclusion, isotope geochemistry and metallogenic acid–alkali geochemical barriers, and iv) different prospecting methods to those typically used for MVT deposits. The Huize-style and typical MVT deposits constitute the carbonate-hosted non-magmatic epigenetic hydrothermal-type (CNHT) Zn–Pb deposits.

KEYWORDS

typical geological-geochemical characteristics, rich Ge-Ag-bearing Zn-Pb deposit, Sichuan-Yunnan-Guizhou Triangle area(SYGT), Huize-style deposit, deposit classification, new model

1 Introduction

The well known Sichuan–Yunnan–Guizhou Triangle (SYGT) of Zn–Pb deposits in southwestern (SW) China is located along the SW margin of the Yangtze Block and is composed of the northeast (NE) Yunnan, northwest (NW) Guizhou, and SW Sichuan deposit concentration districts. Most deposits are distributed across the SYGT area, enclosed by the south–north-trending Xiaojiang fault belt, the NW-trending Kangding–Yiliang–Shuicheng fault belt, and the NE-trending Mile–Shizong–Shuicheng

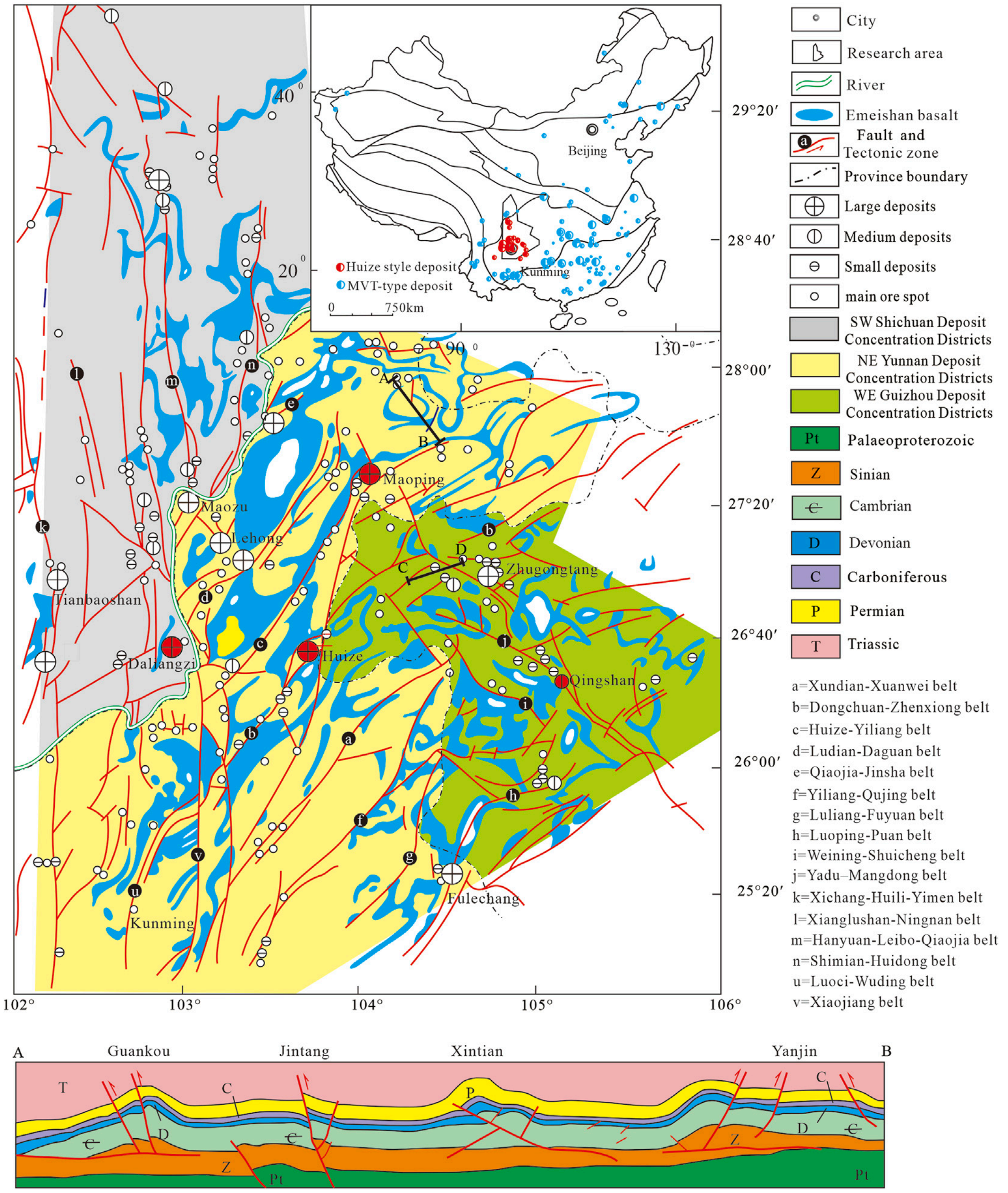

FIGURE 1
Tectonics and distribution map of (Ag–Ge)-Zn–Pb deposits in the SYGT (Modified according to Liu and Lin, 1999) AB is a seismic interpretation profile of the Guankou–Yanjing area (after Southwest Petroleum Survey Bureau, 2000). **(A–H)**: major NE-trending oblique strike-slip fault-fold belts; **(I–J)**: major NW-trending diagonal tensile strike-slip fault-fold belts; **(K–V)**: major SN-trending sheer fault belts.

fault belt (Han et al., 2012a). To date, more than 450 rich Ge-Ag-bearing polymetallic Zn–Pb deposits and mineralised occurrences have been identified in the SYGT, including two super-large, nine large, and 50 medium-large deposits (Han et al., 2007a; Han et al., 2012b) (Figure 1). The SYGT area has become one of the largest potential metallogenic provinces in China and is one of 16 prospecting areas for China Geological Survey Planning. Yunnan Chihong Zn & Pb Co. Ltd. has been established as an international industrial Zn–Pb and Ge resource supplier.

For decades a number of views have emerged regarding the genesis of the SYGT deposits. Before 1999, stratabound genetic viewpoints dominated, including the following: sedimentary-reworking type (Tu, 1984; Tu, 1987; Tu, 1989); hot-water sedimentary type (Zhang, 1984); sedimentary origin closely associated with microfacies carbonates (Chen, 1984); Emeishan basalt magmatic-hydrothermal mobilisation and enrichment during the Indosinian–Yanshanian tectonic localisation (Shen, 1988); rift-related tectonic and rift transformation-reworking (Zhang and Yuan, 1988); deeply circulating geothermal water filling and epigenetic stratabound (Zhong and Mucci, 1995); sedimentation-reworking (Zhao, 1995); sedimentation, reworking and epigenesis (Liu and Lin, 1999); convection-circulation

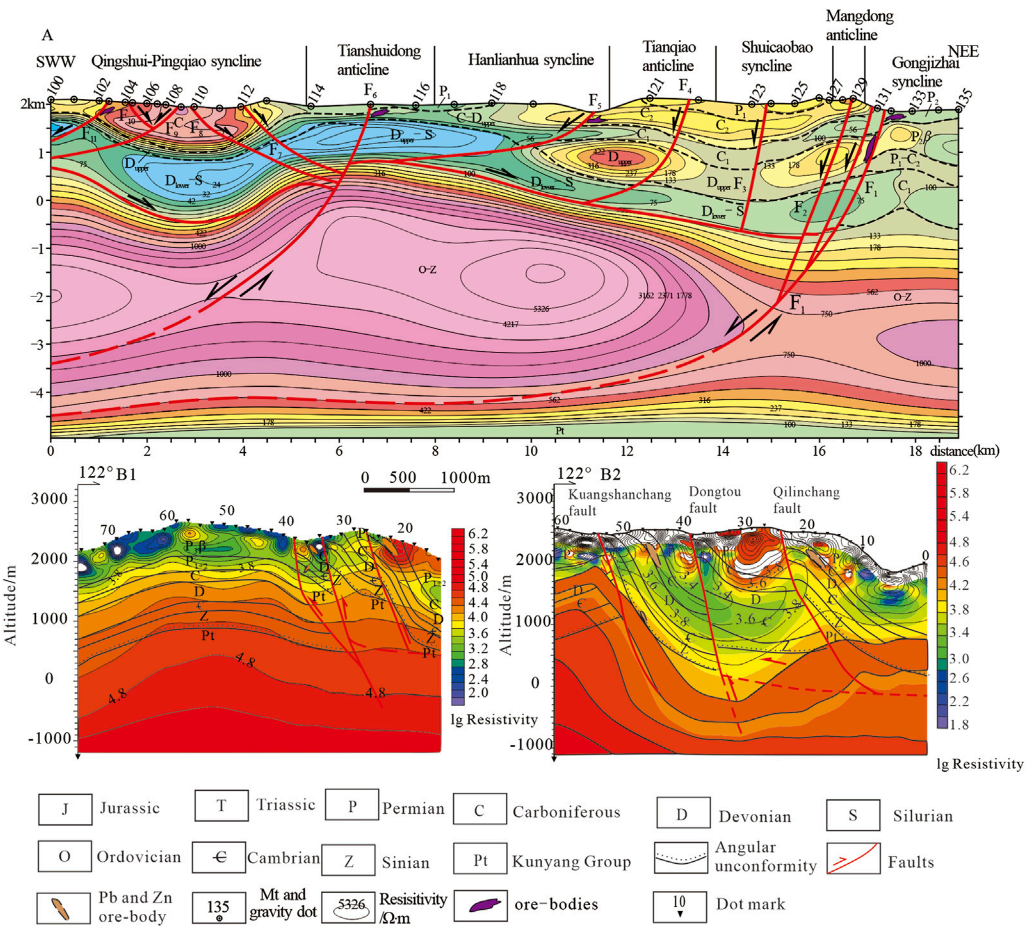

FIGURE 2
(A) The electromagnetic exploration profile of the Yadu–Mangdong belt; **(B)** Interpretation charts of measurement results for exploration lines No. 59 (B1) and No. 129 (B2) in the Huize district.

metallogenesis and hydrothermal caves (Zhen, 1997); and stratabound, epigenetic, and hydrothermal deposition in magnesia carbonates from a neritic platform facies (Zhang, 1989), among others. Subsequently, Han et al. (Han et al., 2001a) proposes that the Huize deposit can be categorised as epigenetic deposits that formed from structurally controlled fluids of deep origin 'injected' into structures. Zhou et al. (2001) classifies the Huize deposit as Mississippi Valley Type (MVT) Pb-Zn deposits hosted mainly by dolostone and limestone within carbonate sequences. Zhai et al. (2011) classify the deposits as hydrothermal stratabound-type deposits.

In general, district-scale extensional faults control the MVT deposits, which are closely linked to contractional events from adjacent orogenies (Leach et al., 2001; 2010; Bradley and Leach, 2003; Hossini-Dinani and Mohammad, 2021) and dominated by hydrothermal filling. However, based on the accumulation of geological data and comprehensive investigations of SYGT deposits, previous studies have shown that an intracontinental oblique strike-slip structure system invariably controls the locations of deposits and ore-bodies, reflecting a compressive structural setting that differs from the typical MVT Zn–Pb ore-forming extensional domain tectonic setting in passive margins, with mineralisation dominated by hydrothermal replacement. At the same time, these deposits have high-grade Zn–Pb ores, reaching averages of up to 15%–35% and even up to 50%, as well as an association with Ag and other dispersed elements, such as Ge, Ga, and Cd. This differs from classic MVT deposits, which are generally of a lower grade (Zhang et al., 2019a). Based on geological data, exploration, a detailed review of the Huize and Maoping Zn–Pb districts, and thorough study of typical deposits in the SYGT (e.g., the Maozu, Fulechang, Lehong, Songliang, Lemachang, Tianbaoshan, Zhugongtang, Tianqiao, and Qingshan deposits), previous studies have observed that these deposits have distinct geological characteristics (Han et al., 2001b; Han et al. 2007a; Han et al. 2012a). Rich Ge and Pb-Zn mineralisation characterise in the intracontinental strike-slip tectonic system, which is due to collisional processes that occurred between the Yangtze and Indosinian blocks during the Late Indo-Chinese epoch. These processes drove deep-origin fluids along the strike-slip fault-fold belt, triggering abnormally high hydrostatic pressure which caused massive fluid flow migration into the fault-fold structure. Owing to multiple coupling processes in terms of tectonics and fluid dynamics, 'injection' and immiscible processes of ore-forming fluids, mixing of

TABLE 1 Statistical results of (Ge–Ag)–Zn–Pb deposits and prospects in the SYGT.

Ore-hosted strata and lithology	Scale and quantity of deposits							Scale and grade of typical deposits (district)/mineralized points
	Large	Medium	Small	Occurrences	Mineralized points	Total	Percentage of the total number of deposits and prospects/%	
Triassic marl and limestone sand and mudstone					3	3	0.74	Mineralized points
Lower Permian Emeishan basalts					1	1	0.24	Mineralized points
Permian dolomitic limestone	3		3	9	8	23	5.66	Fulechang (L, 0.6 Mt@ 15%–25%), Lemachang (L), Zhugongtang (SL, 2.73 Mt@ 10%–25%)
Carboniferous medium-coarse crystalline dolomite and dolomitic limestone	2	3	14	39	12	70	17.25	Huize (SL, total 8.6 Mt@30%–35%, Ge ~1,200 t and Ag ~2000 t), Maoping (SL, total 3.8 Mt@ 15%–30%, Ge ~400 t and Ag ~200 t), Qingshan (M, 0.2 Mt@ 25%–30%), Tianqiao (M, ~0.2 Mt@ 15%–20%)
Upper Devonian medium-coarse crystalline dolomite	1	1	7	20	30	59	14.53	Maoping (SL, total 3.8 Mt@ 15%–30%)
Silurian limestone and sandstone-mudstone		1	5	3	5	14	3.45	Baoxing (M)
Ordovician dolomite and dolomitic limestone		2	2	9	26	39	9.60	Botuowuyi (M)
Cambrian silicified limestone, dolomitic limestone, and sandstone-mudstone	2	1	3	26	41	71	17.49	Wuzhishang (L, 1.53 Mt@ 6%) Daliangzi (L) and Laolin (M)
Upper Sinian dolomite and sandstone-mudstone	3	7	15	28	55	108	26.60	Maozu (L, ~0.8 Mt@ 15%–20%), Songliang (M, 0.1 Mt@ 15%–20%), Lehong (L, 1.2 Mt@ 15%–25%), Tianbaochang (L, 1.1 Mt@ 10%–15%)
Proterozoic Kunyang group and Huili group dolomite	1		3	5	9	18	4.44	Xaoshifang (L), and Huize Laoyinqing (S)

Notes: SL-super-large sale, L-large-sized scale, M-middle-sized scale, S-small-sized scale.

deep-origin fluids and basin fluids, and repeated fluid-rock reactions may all have led to the formation of extensive Ge-Ag-bearing Zn–Pb deposits in the SYGT. Therefore, the formation of these deposits generally occurred over three phases: 1) formation and driving of strike-slip fault-fold belts and large-scale fluid migration; 2) ore-forming fluid 'injection', fluid-rock reactions, and multiple coupling processes between the tectonics and fluid; and 3) unloading of the rich-ore fluid and subsequent mineralization (Han et al., 2012b; Han et al., 2022).

The main findings discussed in this research are as follows: typical characteristics and classification of Huize-style rich Ge–Ag-bearing Zn–Pb deposits in the SYGT; ore-controlling regularities in intracontinental strike-slip fault-fold structures and the tectonic background of metallogenic dynamics; mineralisation periods and supernormal enrichment mechanisms.

2 Geological setting

The SYGT area is adjacent to the south side of the Longmen Shan thrust belt, Nanpanjiang–Youjiang oblique strike-slip belt, and the north side of the Ailaoshan orogenic belt (Luo, 1985; Ma et al., 2004; Qiu et al., 2016; Yan et al., 2018). This area is characterised by a complex geological setting and strong multi-period structural superposition. Complex mechanisms of

10.3389/feart.2023.1136397

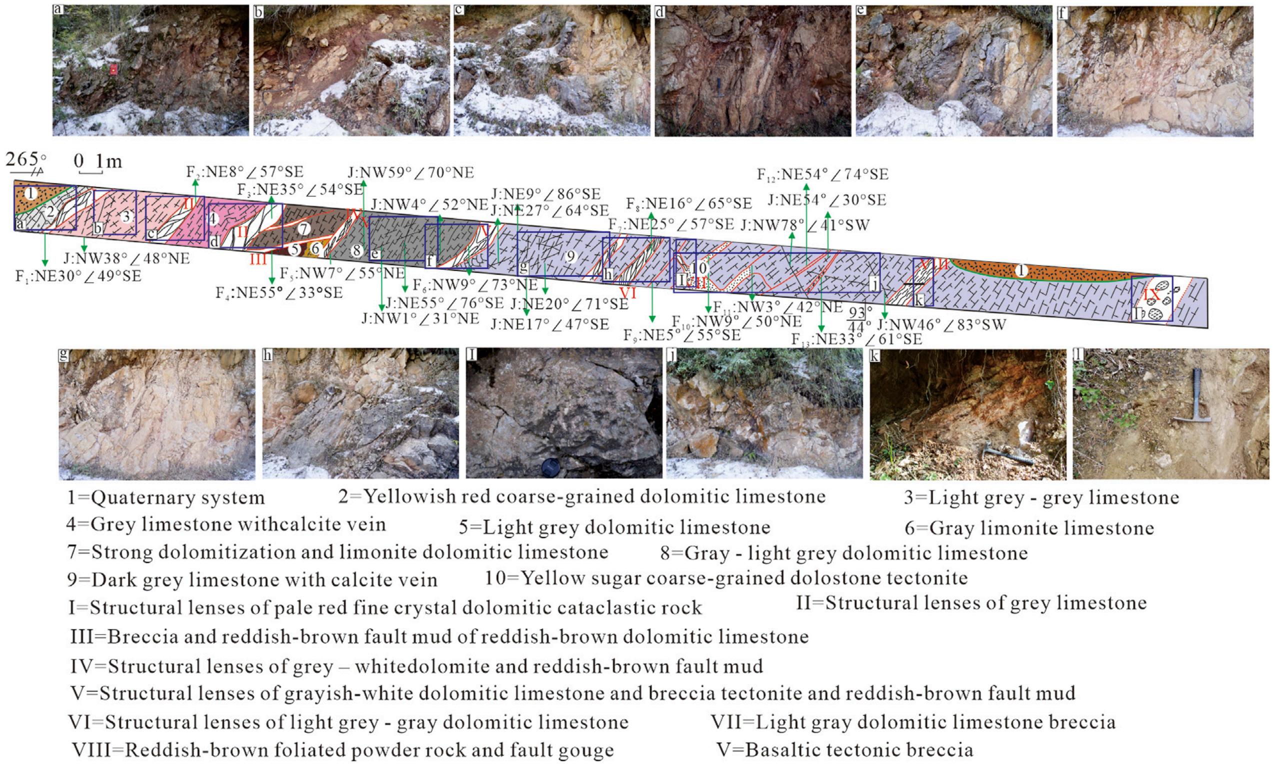

FIGURE 3
Qilinchang oblique strike-slip structure in the Huize ore district (NEYD).

metallogenic dynamics and favourable ore-forming conditions led to the formation of a series of large and super-large Zn–Pb polymetallic deposits (Han et al., 2012a).

2.1 Stratigraphy

The SYGT has a old geological and tectonic history, with a double-layer structure composed of a lower basement and overlying cover (Han et al., 2014). The basement consists of the middle–lower Proterozoic Kunyang Group (1,800–1,000 Ma) and Dahongshan Group (2,500–1,800 Ma) (Fang, 2014) formations. Among them, shallow-marine carbonate-dominated and fluvial siliciclastic-dominated rock formations dominate the low-grade metamorphic greenschist-facies Kunyang Group (Greentree et al., 2006; Han et al., 2006). The cover is composed of upper Proterozoic, Upper Sinian (850–700 Ma) (Fang, 2014), and Palaeozoic strata. Upper Proterozoic rocks include a Lower Sinian igneous suite of mainly volcanic rocks and the Upper Sinian Dengying Formation of marine dolomite. Palaeozoic strata are comprised of Middle–upper Devonian, Carboniferous, and Permian rocks (Liu and Lin, 1999). The Sinian, Devonian, Carboniferous, and Permian carbonates are the primary host rocks of the Zn–Pb deposits. In these strata, the lower Carboniferous Baizuo Formation (Fm.; C_1b), upper Devonian Zaige Fm. (D_3zg), and Upper Sinian Dengying Fm. (Zb*d*) carbonates are the most important host rocks. In the Huize district, argillaceous dolomitic limestone intercalated with thin-layered barite-bearing evaporite in the middle parts of C_1b is lithologically similars to the wall rocks of the MVT deposits. Therefore, we presume that the Huize district was situated within a lagoonal environment and positioned between tidal flat and inter-beach environments in a region of extensive marine sedimentation during the Carboniferous Period. Ore host rocks in other districts of the SYGT formed in similar sedimentary environments. The exposed late Permian Emeishan basalts are the only igneous rocks in the SYGT.

We note that the middle–upper parts of C_1b and D_3zg mainly consist of greyish-white, yellowish-red, cream-coloured, and coarse crystalline dolomite, whereas its middle–lower parts are mainly composed of compact light grey massive limestone and argillaceous dolomitic limestone. When comparing the compressive and shearing strength, dolomite in the middle–upper strata is noticeably weaker than limestone in the middle–lower strata. The strength of parallel bedding directions is significantly lower than that of the vertical bedding directions, which more easily results in interlayer faults within the dolomite (Han et al., 2001b). Consequently, ore-controlling interlayer fault zones likely formed in specific positions within the dolomite. Here, Zn–Pb deposits with dolomite and limestone-bearing dolomite in the Dengying and Maokou Fms. Are similar in their mechanisms.

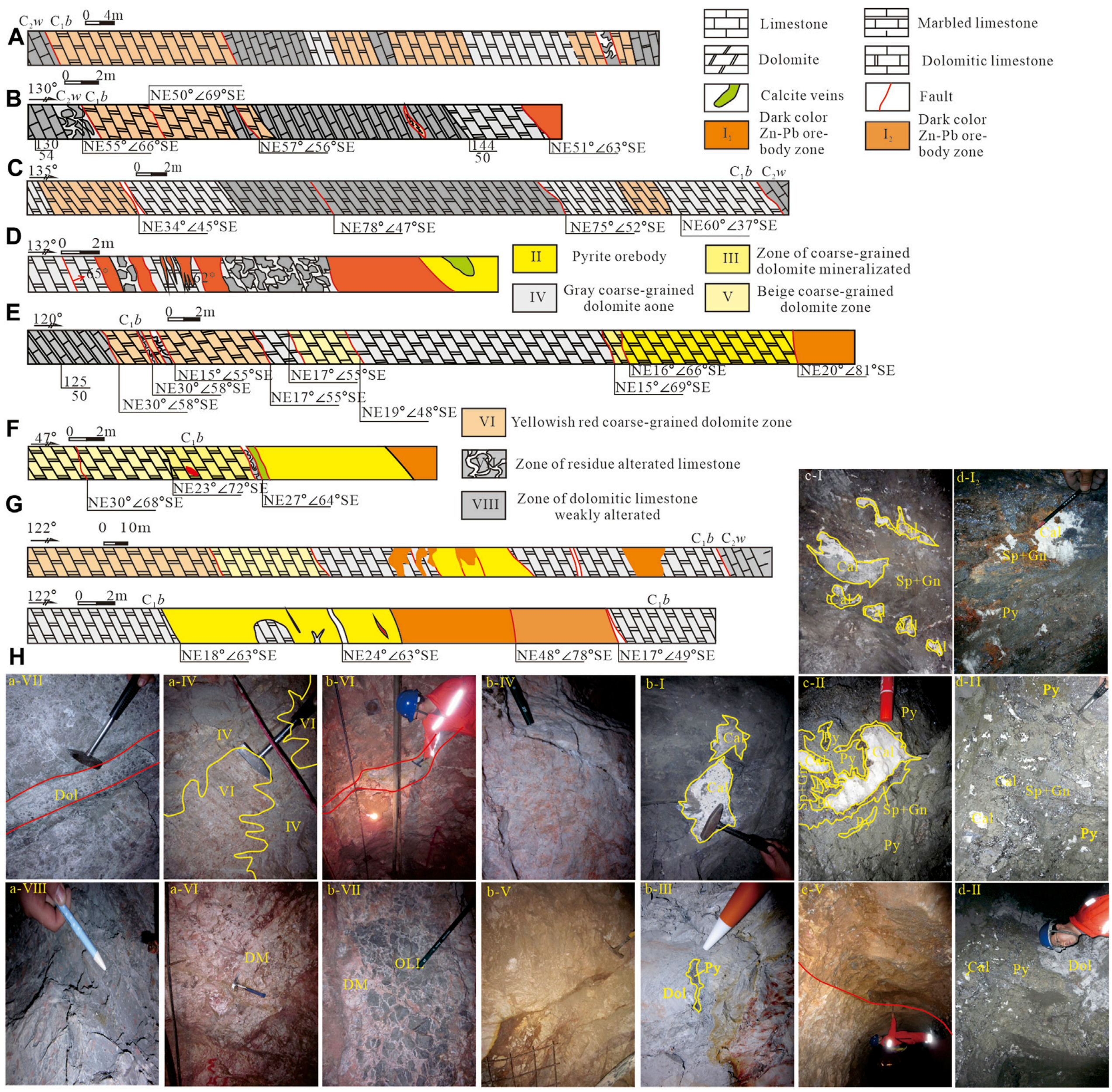

FIGURE 4
Composite assemblage zoning profile of alteration and mineralization in the Huize deposit **(A)**. Horizontal drilling mapping of the No. 73 exploration line at the 1764 m level; **(B)**. No. 11 ore-out tunnel mapping at the 1,584 m level; **(C)**. Transverse tunnel mapping of the No. 26 exploration line at the 1,584 m level; **(D)**. Tunnel mapping of the No. 110 exploration line at the 1,571 m level; **(E)**. No. One ore-out tunnel mapping at the 1,331 m level; **(F)**. No. One ore-out tunnel mapping at the 1,284 m level; **(G)**. Transverse tunnel mapping of the No. 82 exploration line at the 1,261 m level; **(H)**. Transverse tunnel mapping of the No. 90 exploration line at the 1,261 m level; The meaning of the code in the upper left corner of the photo: small letters-No. of transverse tunnel; Roman alphabet: the code if alteration zoning. For example, a-VI represents a typical photo of VI alteration zone in tunnel A.

2.2 Structure

Based on structural geological mapping (Figure 1) (Han et al., 2007a; Han et al., 2012b; Han et al., 2014), an analysis of seismic exploration data (Figure 2), and ore-field structural research, we can show that the intracontinental strike-slip tectonic classification system controls SYGT mineralisation in different areas; that is, the deposit concentration districts, ore deposits (ore-field), and ore-bodies (veins). At a regional scale, the strike-slip fault-fold group controls the SYGT mineralisation area, including the Zn–Pb polymetallic deposit concentration districts, such as the NE Yunnan (NEYD), NW Guizhou (NWGD), and SW Shichuan Deposit (SWSD). The NE-trending oblique upward strike-slip belts control the NEYD, the NW-trending diagonal fall strike-slip belts control the NWGD, and the north–south-trending sheer fault belts

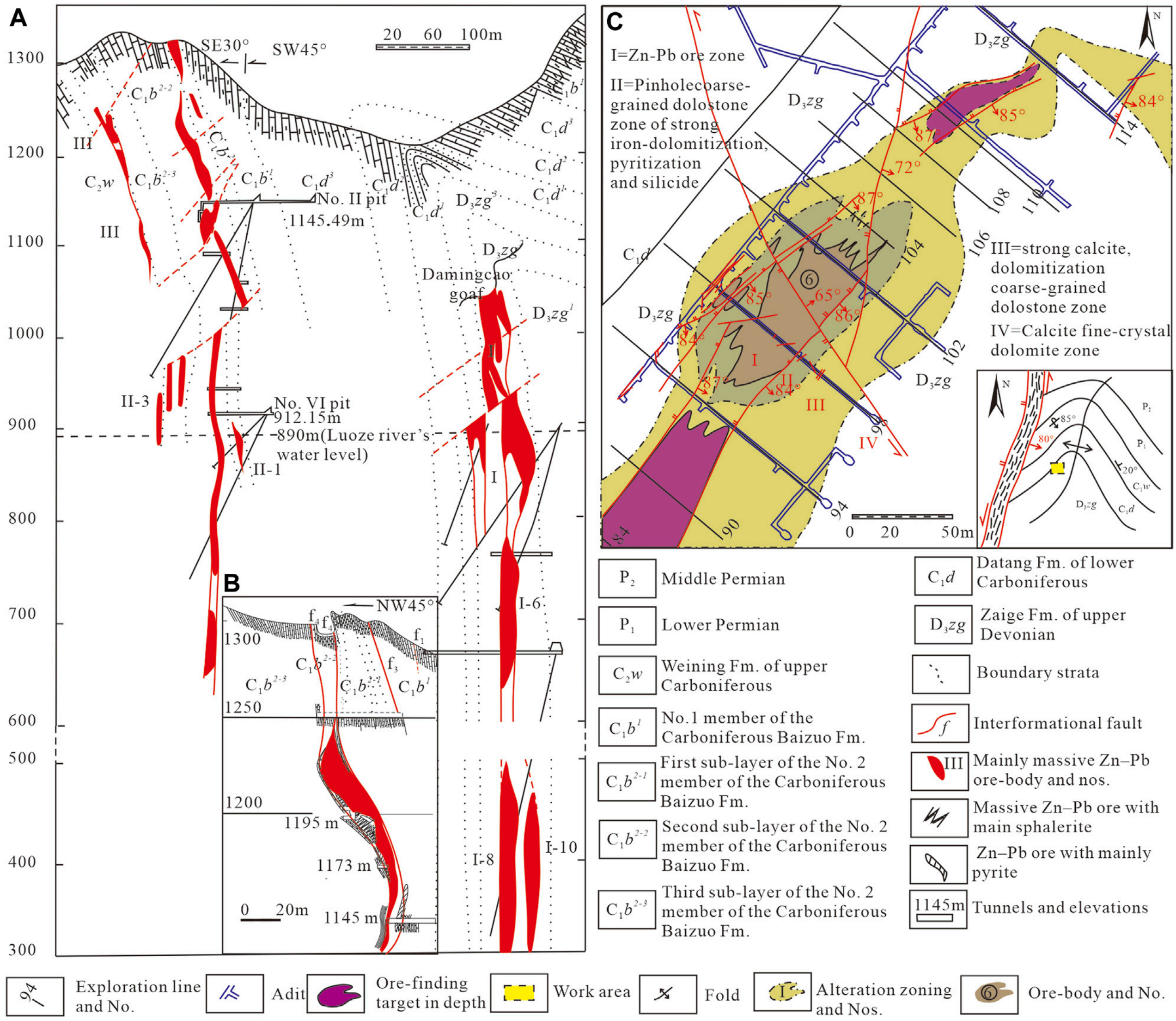

FIGURE 5
(A) Ore-body profile map of the Maoping Zn–Pb deposit; **(B)** Section diagram of the No. Two ore-body group of the Maoping deposit; **(C)** Zonation diagram of mineralization and alteration-lithofacies at the 670 m level in the Maoping deposit.

control the SWSD. At the ore district or smaller scales, a single strike-slip fault-fold structure may control an ore-field or deposit while secondary fault zones or their assorted components may control the ore-bodies or veins.

In the NEYD, there are eight oblique strike-slip belts that compose a NE-trending structural group (Han et al., 2007b; Han et al., 2012a) (Figure 1). These are the Xundian–Xuanwei, Dongchuan–Zhenxiong (also referred to as the Jinniuchang–Kuangshanchang belt in the Huize district), Huize–Yiliang, Ludian–Daguan–Yanjin, Qiaojia–Jinsha, Yiliang–Qujing, Luliang–Fuyuan, and Luoping–Puan belts. Just as the Dongchuan–Zhenxiong belt controls the Zn–Pb ore-field, composed of the Huize, Yulu, and Daibu deposits, the Qilinchang–Kuangshanchang and Yinchanpo oblique strike-slip structures control the Huize Kuangshanchang and Qilinchang large and Yinchangpo middle Zn–Pb districts (Han et al., 2007a; Han et al., 2012b; Han et al., 2015) (Figure 1). Secondary NE interstratified compression-shear faults in altered dolomite zones of the upper plate of the Kuangshanchang–Qilinchang–Yinchnagpo fault directly control the rich and thick ore-bodies (Han et al., 2012a; Han et al., 2014). The Huize–Niujie belt controls the Maoping Zn–Pb district, which is composed of the Fangmaba, Maoping, and Tuogumei deposits (Han et al., 2012b). These NE-trending oblique strike-slip belts have developed into a complicated ore-controlling system, which has been documented as a typical xi-type structural tectonic pattern (Han et al., 2001a; Han et al., 2006).

The structural system of the NEYD is composed of major components, including NE-trending anticlines with sinistral ore-bearing interstratified faults (which control the Huize, Maoping, Fule, and Maozu deposits, among others), as well as other assorted components, including NW-trending high-angle tension-shear faults and SN-, NNW-, and EW-trending shear faults. The average orientation of the principal compressive stress axis (σ_1) was NW–SE

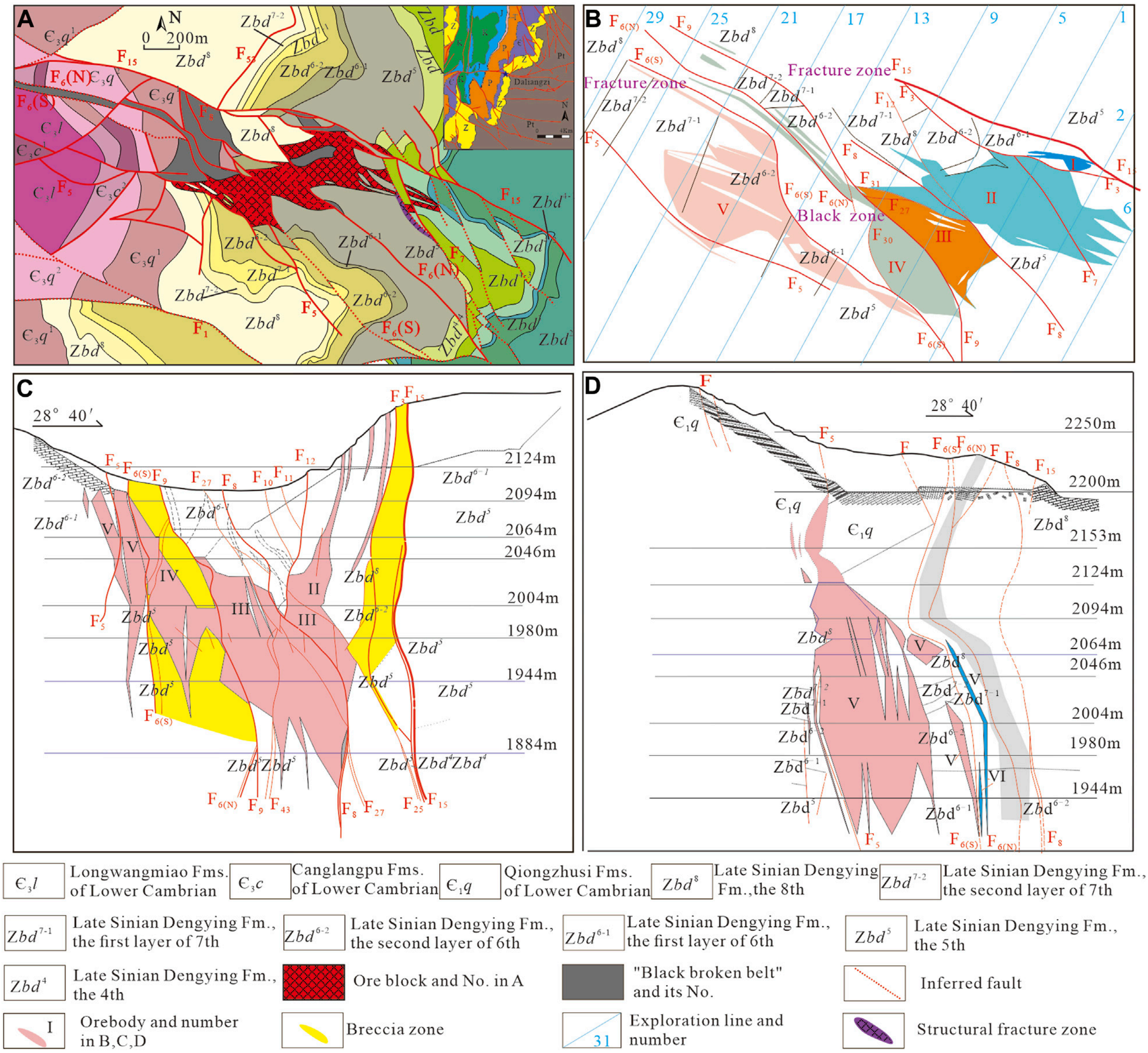

FIGURE 6
(A) Geological map of the Daliangzi lead-zinc deposit; **(B)** Distribution map of black belt and ore block in 2004 m level in Daliangzi Pb-Zn deposit (redrawn according to mine data); Profile of exploration line **(C, D)** of the Daliangzi Pb-Zn deposit (according to mine data).

during the Zn-Pb mineralisation period. The NE-trending folds and sinistral compression-shear faults were the main conduit structures of the ore-forming fluid migration while the NW-trending tension-shear faults were ore-matching structures. The lower-order NE-trending interstratified fault zones were also the main ore-allocation or ore host structures and appear as an echelon fracture group, identified as xi-type structures (on a plane) or stepped-type (along profile) ore-controlling structures (e.g., the Huize and Maoping deposits) (Han et al., 2012a; Han et al. 2014; Han et al. 2015).

There are four strike-slip fault belts in the SWSD, establishing a SN-trending structural group, including the Xichang–Huili–Yimen, Xiangluoshan–Ningnan, Hanyuan–Leibo–Qiaojia, and Shimian–Huidong belts. The Xichang–Huili–Yimen belt (Han et al., 2014) (Figure 2) controls the Tianbaoshan Zn–Pb-(Cu) Zn–Pb deposits, among others.

There are also two diagonal tensile strike-slip fault-fold belts in the NWGD, making up a NW-trending structural group, including the Weining–Shuicheng and Yadu–Mangdong belts (Figure 2) (Han et al., 2014). The former controls the Qingshan, Shanshulin, and Shangshiqiao medium-sized deposits while the latter controls the Zhugongtang super large-sized deposit and a series of medium-sized deposits, including the Yadu, Xiaojiwan, Zazichang, Maomaochang, and Tianqiao deposits (Figure 1).

2.3 Magmatism

There are up to 52 igneous outcrops of intermediate to basic-ultrabasicity rocks along the NS-trending Xiaojiang fault zone of the SYGT (Yuan et al., 1985b; Song et al., 2001). There is, however, only

 10.3389/feart.2023.1136397

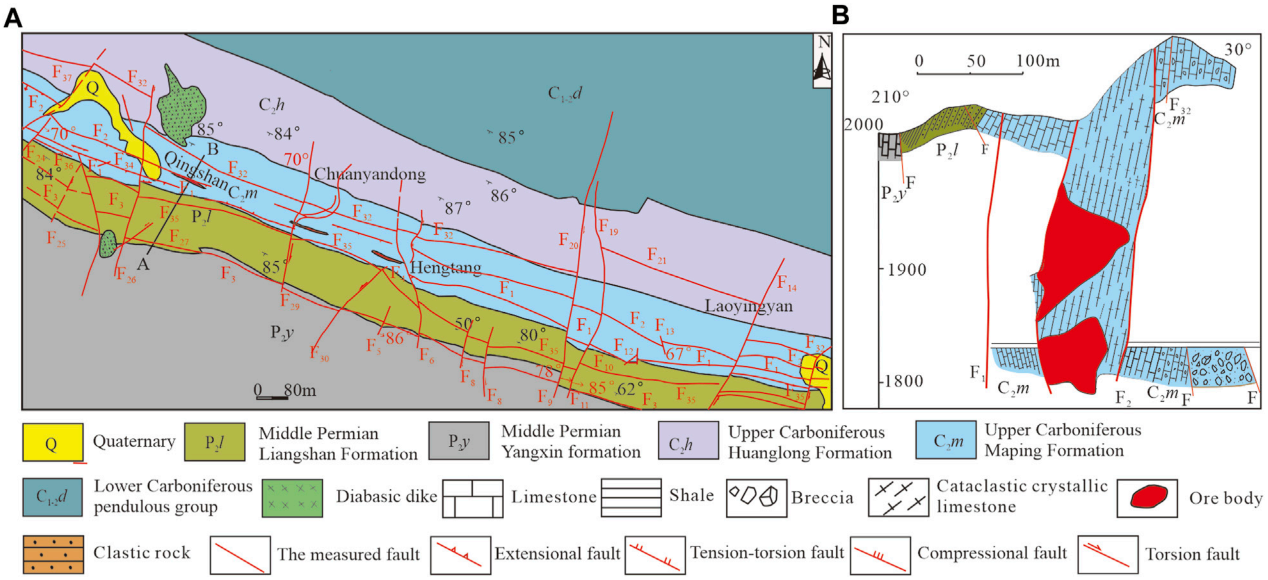

FIGURE 7
(A) Simplified geological maps of the Qingshan lead-zinc deposit; **(B)** Orebody profile of the Qingshan lead-zinc deposit.

one location where pyritised ultramafic rocks supported Pb and Zn mineralisation. These diabase and gabbro-diabase sills and dikes (K–Ar ages: 246–283 Ma) lie on the eastern side of the Xiaojiang fault (Liu and Lin, 1999). Certain diabase contact zones experienced intense hydrothermal alteration (e.g., silicification and epidotisation) and Pb, Zn, and Cu mineralisation.

Late Permian Emeishan basalt (K–Ar ages: 218.6–253.3 Ma; Zircon U–Pb age: 258.6 Ma) (Yuan et al., 1985a; Cong, 1988; Zhou et al., 2002; Guo et al., 2004; Zhong and Zhu, 2006; Zhou et al., 2006; Tao et al., 2009) is vital when attempting to understand local magmatic activity. The basalt may spatially coincide with Zn–Pb-(Ag–Ge) deposits and ore occurrences (Figure 1), but is not related to Zn–Pb metallogenesis (Han et al., 2012b).

3 Geology of typical main deposits

In the past 25 years, we have been studying over more 20 deposits which are this type of lead-zinc deposits in the Sichuan-Yunnan-Guizhou metallogenic area and accumulated a lot of data. Due to limitation of the length of an article, we select the four most representative deposits.

3.1 Huize super-large ore district

This district, which is one of richest super-large rich Ge–Ag-bearing Zn–Pb deposits worldwide and typical of the NEYD (Figure 1; Table 1), is situated at the eastern side of the Xiaojiang fault belt and comprised of the Kuangshanchang, Qilinchang, and Yinchangpo deposits, located 40 km from Huize town, which has supported mining in both ancient and present times (Han et al., 2006). Numerous advances have occurred, especially in terms of deposit geology (Liu and Lin, 1999; Han et al., 2006; Han et al. 2007b; Han et al. 2012a; Han et al. 2014; Han et al. 2015; Han et al. 2016). Therefore, we focus on the characteristics of the tectonic mineralisation and alteration, which have received less attention in previous studies.

The Huize Zn–Pb ore district controlled by the NE-trending Dongchuan–Zhenxiong oblique strike-slip belt tectonically, which resulted from sinistral shear of the Xiaojiang fault, while the Maoping–Qujing concealed the fault during the Indosinian orogeny period (Figure 1). In general, deposits in this district are controlled by NE-trending Kuangshanchang, Qilinchang, and Yinchangpo fault-fold structure series, as confirmed by magnetotellurics exploration (Figure 2B) and ore-forming structural analysis (Figure 3).

The major faults in the NEYD have experienced multiple movements and are spatially related to the Zn–Pb-(Ag–Ge) orebodies (Han et al., 2015). There are five orientation faults in the district: the NE-, NW-, NNW-, ‘north–south-, and east–west-trending faults. From the late Permian to Middle–Late Triassic, crustal movements changed from extension to compression strike-slip. The north–south-, NE-, and NW-trending tectonic zones formed during the Triassic Indosinian orogeny period (230–200 Ma).

The NE-trending ore-controlling faults led to the development of various types of tectonites, including clastic, clast-porphyritic, mylonite, and cataclastic tectonites with different textures (Figure 3). For example, the Qilinchang fault zone developed Zn–Pb mineralised tectonic lenticels and foliated cataclastic belts, which led to widespread hydrothermal alteration of ferrous dolomitisation and pyritisation (Figure 4). In contrast, other trending faults are mostly associated with a single type of tectonite (i.e., mainly cataclastic). NE-trending ore-bearing interlayer fractures result in SW-trending lateral dip of the orebody group.

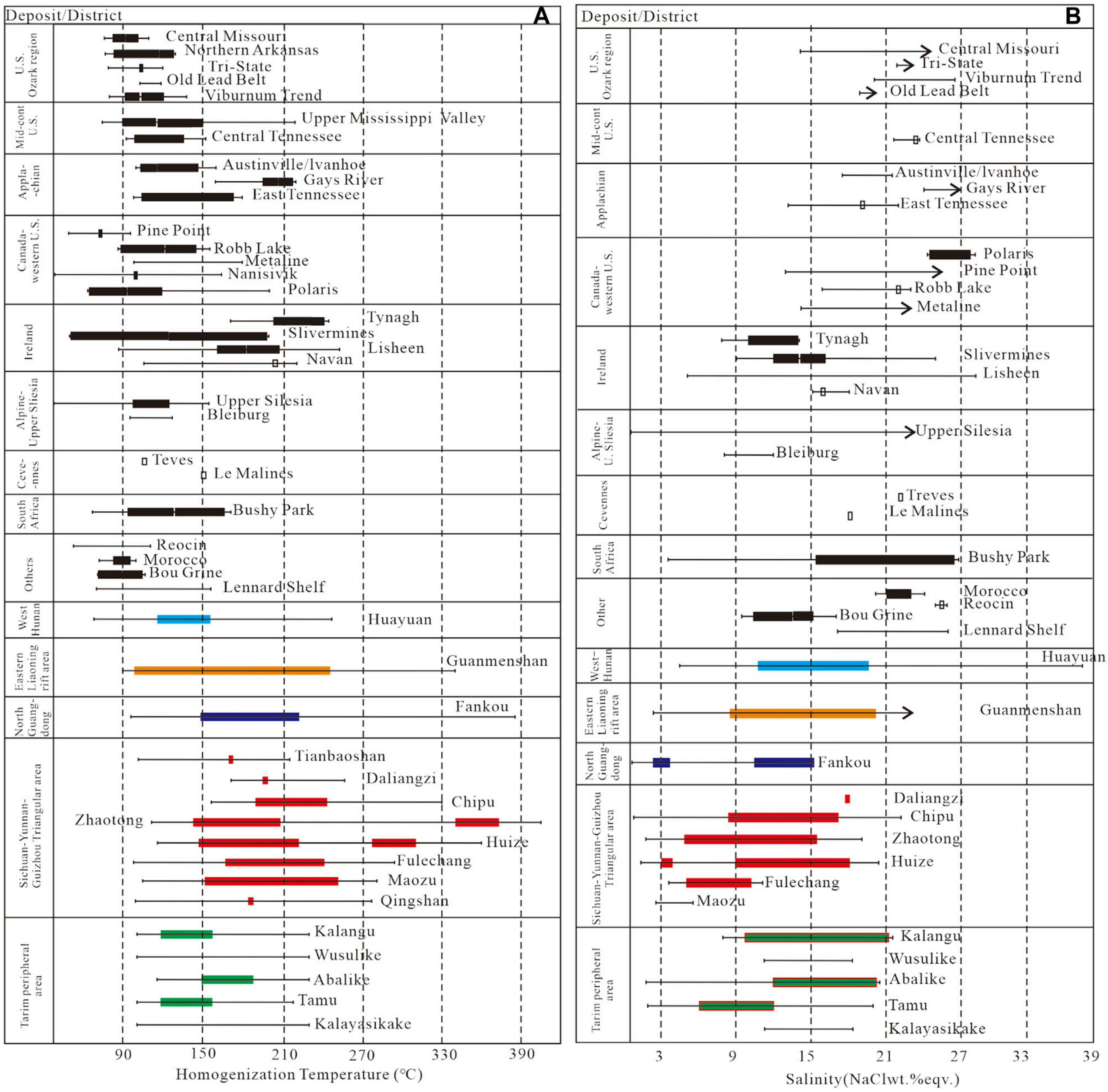

FIGURE 8
Homogenization temperature **(A)** and Salinity **(B)** distribution of ore-forming fluid inclusions in mainly Zn-Pb deposit both in China and abroad Data from (Rui et al., 1991b; Liu and Zheng, 2000; Wang et al., 2002; Kuang et al., 2003b; Leach et al., 2005; Gao, 2006; Feng et al., 2009; Zhu et al., 2013).

Hydrothermal alteration results in an intense water-rock reaction along ore-controlling fault zones. As shown in Figure 4, across the ore-controlling oblique fault zone upward to the ore-hosting rocks, mineral assemblage zoning and alteration shows that associations of alteration and mineralisation occur in the following order: barite + pyrite + quartz zone in the Kuangshanchang fault → weakly dolomitised limestone zone (VIII) → net veined coarse-grained dolomite with residual calcitised fine-crystalline calcareous dolomite zone (VII) → reddish medium-coarse crystalline dolomite zone (VI) → beige pinhole-like coarse crystalline dolomite zone (V) → grey coarse-grained dolomite zone (IV) → star-like Zn–Pb and pyrite-mineralised porous coarse crystalline ferro-dolomite zone (III) → (lower surface of interlayer fault belt) Zn–Pb mineralised pyrite zone (II) → (Zn–Pb ore zone (I1; dark grey sphalerite + densely disseminated pyrite zone → sphalerite + galena + pyrite ore zone) → fine-grained pyrite + dolomite + calcite in coarse crystalline dolomite zone (I2; upper surface of interlayer fault belt) → grey-beige impregnated pyritisation hole and pinhole with coarse crystalline ferro-dolomite zone (III–V) → coarse-grained dolomite with small residual limestone zone (VI, VII).

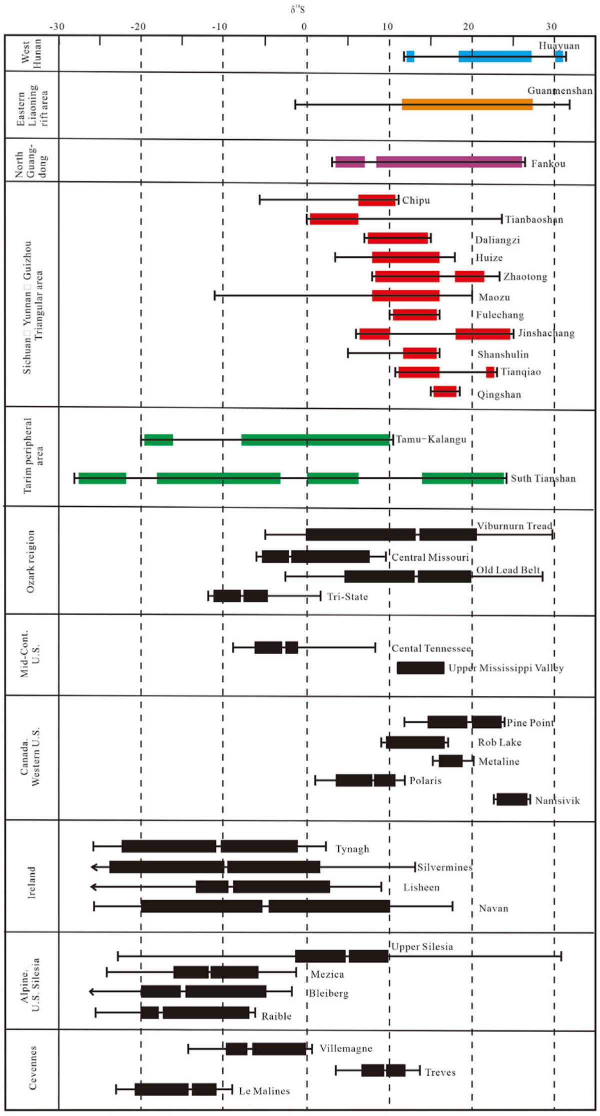

FIGURE 9
Sulphur isotopic composition distribution of metal minerals in mainly Zn–Pb deposits both in China and abroad Data from (Zhou et al., 1983; Chen and Zeng, 1984; Liao, 1984; Peng, 1990; Rui et al., 1991a; Wang, 1991; Xu et al., 1996; Zhou, 1996; Mao et al., 1997; Zhu et al., 1998; Liu and Lin, 1999; Kuang, 2003a; Luo, 2003; Zhang, 2003; Zhu and Zhang, 2004; Han, Chen, Huang, et al., 2006; Gao et al., 2007; Gu, 2007; Xue et al., 2007; Wang, 2008; Xiao et al., 2009; Cong et al., 2010; Dong et al., 2010; Li et al., 2010; Yang et al., 2010; Zhu et al., 2013).

3.2 Maoping super-large ore district

The Maoping district, which is also one of the super-large rich Ge-Ag-bearing Zn–Pb deposits and typical of the NEYD, lies on a structural junction between the NE-trending Huize–Niujie oblique strike-slip fault-fold belt and NW-trending Yadu–Mangdong fault belt (Figure 1; Table 1). This district is composed of the Maoping super-large deposit (controlled by the Maoping fault-fold structure), the Fangmaba small-sized deposit (controlled by the Fangmaba -fold structure), and the Yunluheba medium-sized deposit (controlled by the Daibu fault-fold structure). The primary strata in the district are Devonian, Carboniferous, and Permian. The Proterozoic Kunyang Group is the unexposed base in the district.

Multiple ore-hosting strata, including the Zaige Fm. Of the upper Devonian (D_3zg) and Baizuo (C_1b) and Weining Fms. (C_2w) of the lower–upper Carboniferous, are the typical feature of this deposit. These strata are mainly composed of greyish to white, pinkish, and cream coarse crystalline dolomite; light grey compact massive limestone; and siliceous limestone. The ore-bodies are distributed along the northwest plunging wing of the Maomaoshan overturned anticline, and controlled by the interstratified fault zones which result in SW-trending lateral dip of the orebody group. In this district, the only igneous rock is the upper Permian Emeishan basalt.

The ore-body shapes vary with their spatial distributions, which include large vein, chamber, lenticular, and stratiform shapes, with continual expansion and contraction (Figures 5A,B). The ore grades of Pb and Zn in the Noes. One and six ore-body groups are high (up to 25%–30%), mostly occurring as compact massive ores. In the No. Two and No. Three ore-body groups, the ore grades of Pb and Zn are up to 15%–20%. In addition to being rich in Pb and Zn, the Ag grade can reach 495.6 ppm. The ores also contain other dispersed elements, including Ge (≤203 ppm) and Cd (≤735.5 ppm; Table 1). The mineral composition includes sphalerite, galena, pyrite, ferro-calcite, calcite, and dolomite in the sulphide ores, with minor proportions of quartz and barite. The bead-like and columnar ore-bodies occur at full thicknesses in flat fault areas and thin thicknesses along steep faults, stably extending to an elevation of −38 m (Figures 7, 8). Ore-forming processes have been divided into the hydrothermal ore-forming period (including pyrite-sphalerite, sphalerite-galena-pyrite, and calcite-pyrite stages) and the epigenesis period (Han et al., 2007b). Mineral zoning and alteration from ore-bodies to wall rocks occurs in four parts (Figure 5C): Zn–Pb ore zone (net vein and dense, massive Pb-Zn ore zone) → ore-nearing zone (pinhole with coarse crystalline dolomite zone with strong ferrous dolomitisation-pyritisation) → transitional zone (coarse crystalline dolomite zone with strong dolomitisation and calcitisation) → peripheral zone (fine-crystalline dolomite zone with calcitisation).

3.3 Daliangzi large-sized Zn–Pb deposit

The Daliangzi district, which is one of the large Zn–Pb deposit and typical of the SWSD, is located in the NWW–EW-trending right-hand strike-slip fault-fold zone between the near north–south-trending Xiaojiang deep fault and the Puduhe deep fault in the ore concentration area of Southwest Sichuan (Figure 6A). The primary strata in the district are dolomite of the Dengying Fms. (Z*bd*; Sinian), sand shale of the Qiongzhusi Fms. (ϵ_1q; lower Cambrian), and epimetamorphic rock series of the Mesoproterozoic basement Huili Group (*P*th). There is a parallel unconformity contact relationship between the Qiongzhusi and Dengying Fms., and unconformity contact relationship between the shallow metamorphic rock series of the Huili Group and overlying Neoproterozoic Lower Sinian carbonate rock series. The ore deposit is obviously controlled by a structural and lithologic combination. The NWW–EW-trending main faults (e.g., F15, F1 and their derived NW-trending faults such as F5,

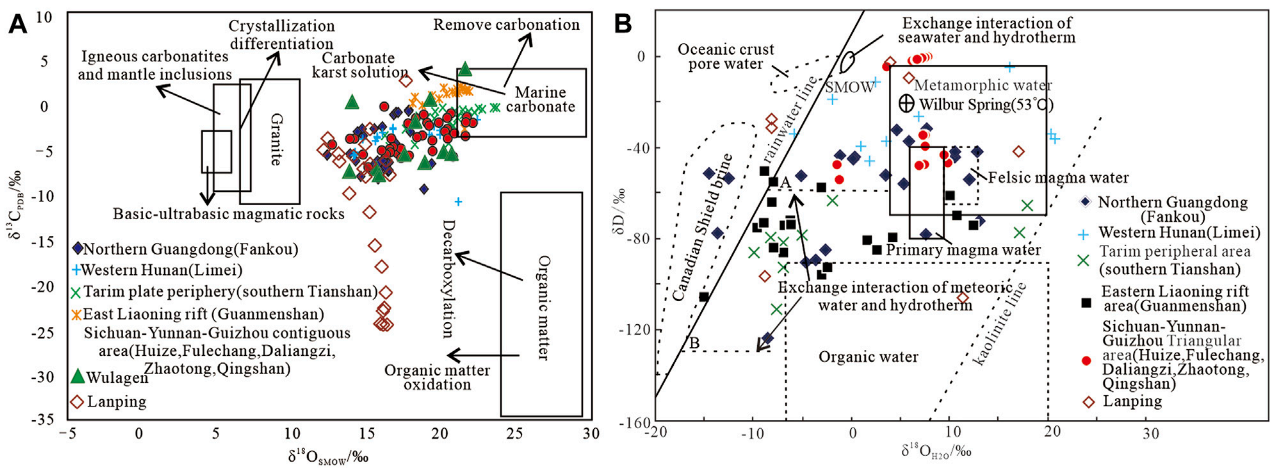

FIGURE 10
Distribution diagram of C-O **(A)** and H-O **(B)** isotopic composition in mainly Zn–Pb deposits both in China and abroad Data from (Chen and Zeng, 1984; Luo, 1995; Xia and Shu, 1995; Lin, 1998; Chen et al., 2000; Kuang et al., 2002; Han et al., 2006; Gao et al., 2007; Yang and Lao, 2007; Zhu et al., 2010; Han et al., 2011a; Li, 2011; Tang et al., 2011; Zheng et al., 2012); (Yin et al., 1983; Wang, 1991; Luo, 1995; Wen et al., 1995; Xu et al., 1996; Zhou, 1996; Liu and Lin, 1999; Han et al., 2006; Han et al., 2007b).

F6, F8 and F9) control the shape and occurrence of the ore-body group; the main host rocks are siliceous dolomite and phosphorous dolomite of the Dengying Fm. (Sinian system), and the upper strata are calcareous fine sandstone, siltstone, and a thin layer of lower Cambrian marl (Figure 6A).

The deposit is composed of the No. 1 and No. 2 ore-body groups; the No. 1 main ore-body group is divided into five blocks (I–V). The ‘black fracture zone’controlled by the F6N and F6S faults divides the main ore-body group into two parts (Figure 6B). The ore block thickness and ore grade in the northeast panel are significantly higher than those in the southwest panel. The ore-bodies in the northeast panel are funnel-shaped (Figure 6C), and are mainly composed of high-grade massive and breccia ores. The ore bodies in the southwest panel have the characteristics of “small in the upper part and large in the lower part” (Figure 6D), and are mainly composed of low-grade vein, fine net vein, and breccia ores. The network vein is the major type. The ore-body strikes the NWW–EW-trending fault, with a length of more than 630 m, inclines to the NE or SW (locally), and has a steep dip angle (>75°). The thickness of the ore body is 0.81–169.79 m (average 52.67 m), and the average grades of Pb and Zn are 0.70% and 10.50%, respectively. The ore structures are mainly massive, brecciated, disseminated, veins and veinlets. The ore minerals are mainly sphalerite, followed by galena. There are also oxide minerals such as plumbite, bauxite, chlorophosphonite, smithsonite, hemimorphite, hydrozinite and sillimanite, along with minerals such as pyrite, chalcopyrite, and Malachite. Gangue minerals are mainly dolomite, calcite, and quartz, followed by sericite, kaolinite, collophanite, chalcedony, barite, and graphite. The main wall rock alteration types include silicification, carbonation, pyritisation, and carbonation. Among them, silicification is mainly represented by vein and disseminated quartz; pyritisation is mainly represented by disseminated and veinlet fine-grained pyrite; carbonation is mainly vein and disseminated calcite and dolomite; carbonatisation is mainly characterised by asphalt and carbonisation, which is widely developed in the’black fracture zone’and the strata fissures of the upper and lower walls of ore the body.

According to the characteristics of vein interpenetration, different altered mineral assemblages, and ore fabrics, the metallogenic process of the deposit can be divided into a hydrothermal metallogenic period and supergene stage. The hydrothermal mineralisation period can be divided into three stages: i. A quartz-pyrite stage, characterised by quartz vein and agglomerate pyrite; ii. A sphalerite-galena-pyrite polymetallic sulphide stage, for which the main ore minerals are sphalerite, galena, pyrite, and smaller amounts of chalcopyrite, tetrahedrite. Gangue minerals are calcite, dolomite, asphalt, etc.; sphalerite is light yellowish brown to orange red, with a euhedral granular structure, and both vein and colloidal structures; galena is common in edge structures with chalcopyrite and tetrahedrite; and iii. Carbonate stage, for which the main minerals are sphalerite, dolomite, calcite, and pyrite; sphalerite is light brown yellow. At a depth of 1,944 m, the homogenisation temperatures of fluid inclusions of sphalerite and calcite for the main metallogenic stage are 146.3°C–288.5°C, with an average of 186.8°C; the salinity is 5.3–18.8 wt% NaCleq., with an average of 11.3 wt% NaCleq. depos

3.4 Qingshan medium-sized Zn–Pb deposit

Qingshan deposit is a typical middle-sized deposits of the SW wing of the Weining–Shuicheng anticline in the middle of the Weining–Shuicheng Pb-Zn sub-metallogenic belt in NWGD. The main exposed strata in the mining area (Figure 7A) are dolomitic limestone of the Baizuo Fms. (C_1b; lower Carboniferous), limestone of the Huanglong Fms. (C_2h; upper Carboniferous), limestone of the

TABLE 2 Element content (ppm) of useful byproducts in ores of the Huize and Maoping deposits.

Associated elements			Cd	Ge	Ga	In	Tl	Ag	Cu	Sb
Huize deposits	Deposits (98)	Range	2.55–1,686	0.520–256	0.495–35.9	0.010–3.82	0.345–305	0.576–309	4.46–2,691	7.58–661
		Average	661	62.1	2.26	0.648	61.2	54.7	204	170
	No. 6 ore-body (42)	Range	31.0–1,686	1.49–224	0.495–7.74	0.024–3.82	9.01–305	7.38–309	5.01–2,691	23.6–661
		Average	687	69.4	1.7	1.15	44.1	83	272	205
	No. 1 ore-body (29)	Range	5.65–1,470	1.66–204	0.637–35.9	0.014–1.63	1.04–70.9	0.576–103	22.3–609	23.4–550
		Average	705	66.8	3.22	0.33	26.2	27.3	177	185
	No. 10 ore-body (27)	Range	2.55–1,256	0.520–256	0.574–5.07	0.010–0.960	0.345–53.0	2.01–160	4.46–538	7.58–316
		Average	574	45.8	2.1	0.22	16.6	40.2	127	99.6
	Enrichment coefficient		3,305	41.4	0.15	6.5	136	781.4	3.7	855
Maoping deposit	Deposit	Range	21.43–735.48	0.97–202.97	0.81–10.14	1.11–4.22	1.48–15.87	29.70–495.55	48.71–1,658.41	8.78–1,306.35
		Average	171.57	24.64	4.81	1.97	4.14	87.89	199.19	235.69
	No. 1 massive ore-body (10)	Range	21.43–735.48	0.97–202.97	0.81–7.2	0.11–3.83	3.28–15.87	41.17–495.55	48.71–1,658.41	100.25–1,306.35
		Average	254.21	39.22	3.26	1.27	6.18	133.63	296.75	395.1
	Nos. 2 and 3 massive ore-bodies (9)	Range	49.96–117.38	3.19–21.83	3.65–10.14	0.493–4.22	1.48–2.72	29.70–80.81	58.77–139.64	8.78–192.31
		Average	88.93	10.06	6.35	2.66	2.1	42.15	101.63	76.27
	Enrichment coefficient		857.9	16.4	0.06	19.7	9.2	1,255.6	3.6	1,178.5
Clarke value *			0.2	1.5	15	0.1	0.45	0.07	55	0.2

Analytical unit: Open Lab. Of Ore Deposit Geochemistry, Institute of Geochemistry, Chinese Academy of Sciences (CAS), P. R. C. Note: the number in brackets reflects number of samples. *After Taylor (1964).

TABLE 3 Physico-chemical conditions of fluid migration stage and unloading stage in the Huize and Maoping deposits (Zhang, et al., 2017a).

Deposit	Physico-chemical conditions of fluid migration stage							
	Homogeneous temperature/°C	Salinity/wt% NaCleq	Pressure/ 10^5Pa	Ore-forming depth/m	pH	$\log f_{O_2}$	$\log f_{CO_2}$	$\log f_{CO}$	Fluid type
Huize	>364	<4.7			<4.9				Ca^{2+}-Mg^{2+}-Na^{+}-Cl^{-}-HCO_3^{-}-CO_2-SO_4^{2-}
Maoping	>352	<4.4	>614		0–6	<-43.4	—	<-44.1	
I (pyrite + ferrodolomite +sphalerite) ore-forming stage in fluid unloading stage									
Huize	173–364 (190–205)	4.7–20.1 (9–11,15–17)			3.7–3.6	51.5~-37.1	−14.1-6.6	−5.8–1.0	Ca^{2+}-Mg^{2+}-Cl^{-}-HCO_3^{-}-SO_4^{2-}
Maoping	168–352 (200–215; 260–300)	4.4–18.0 (9–11)	311–614	1,174–2,317	6–9	−43.4~-29.3		−44.1~-4.1	
II(sphalerite+galena+ pyrite +dolomite)ore-forming stage in fluid unloading stage									
Huize	152–283 (175–190)	2.8–20.9 (14–15)			5.6–5.9	−51.4~-37.3	−14.6–7.0	−6.1–7.2	Ca^{2+}-Mg^{2+}-Na^{+}-Cl^{-}-HCO_3^{-}-SO_4^{2-}
Maoping	152–276 (170–185)	18.0–5.2 (10–11.5)	272–635	1,026–2,398	5–8 (4–5.6)	−48.6~-35.9 (−48.9~-38.1)	(10.9–13.3)	−49.8~-5.1	
III(galena+sphalerite + pyrite + dolomite + calcite) ore-forming stage in fluid unloading stage									
Huize	116–251 (145–160)	1.1–18 (14–17,9–12)			5.1–5.7	−50.6~-41.6	−16.1–10.6	−14.3–8.5	Ca^{2+}-Mg^{2+}-Na^{+}-Cl^{-}-HCO_3^{-}-SO_4^{2-}
Maoping	104–173 (140–165)	19.2–0.8 (10–18)	305–637	1,153–2,406	4.1–7.1	−55.5~-39.8		−56.9~-6.5	
IV(pyrite + dolomite + calcite) ore-forming stage in fluid unloading stage									
Huize	133–213 (130–145)	1.5–7.1 (3–4.5)			5.84–5.85	−50.6~-41.6	−16.1–10.6	−14.3–8.5	Na^{+}-Cl^{-}-HCO_3^{-}-SO_4^{2-}
Maoping	73–172 (100–125)	18.8–1.5 (5–11)	363–562	1,371–2,124	3.1–6.1	−63.1~-54.5		−25~-8.2	

10.3389/feart.2023.1136397

TABLE 4 Comparison of Zn–Pb deposits in the SYGT and typical MVT-type deposits.

Deposit types		Huize-style deposits	Typical MVT-type deposits
Geological processes and ore-forming geological body	Ore-forming structural setting	Intracontinental strike-slip tectonic background in Indonesian collision orogenic processes	Cratonic platform, foreland basin edge, and passive continental margin
	Main controlling factors	Strike-slip fault-fold structures	Normal fault and sedimentary structures including ancient karst, calcium silicon surface, unconformity surface
	Typical features of deposits	High grade of Zn–Pb ores in deposits, large reserves of deposits and ore-bodies, high content of Ge, Ag, Cd, Ga, and In, large extending depth, strong dolomitization, higher mineralization temperature, mineral assemblage and differentiation/alteration zoning	Lower grade of Zn–Pb ores in deposits, large reserves of deposits, lower content of symbiotic components, lower extending depth, weaker alteration, lower metallogenic temperature, no mineralized alteration zonation
	Mineralization horizon	No fixed horizon of mineralization with occurring multi-layers	As a general rule, single layer
	Metallogenic geological bodies	Strike-slip fault-fold tectonic belt controlling mineralization and alteration	Diagenetic carbonate and same period structures
Ore-forming structure	Ore-forming structural system	Northeast-trending structural belt	Combination of sedimentary structure and extensional fault systems
	Ore-forming structure	fault-fold zone and interface of alteration-lithofacies	Ancient karst, calcium silicon surface, unconformity surface, uplift of the basement, and normal fault
Features of ore-forming fluid	Ore structure	Block, vein, reticulated vein structures and replacement textures	Crusty, dissolved breccia structures and packing texture
	Physical-chemical conditions	183–221°C; 250–355°C	75–150°C, mainly distributed at 150–240°C in China
		(13–18)wt% $NaCl_{eq}$; (1.8–4) wt% $NaCl_{eq}$	(15–35) wt% $NaCl_{eq}$
		Acidic to neutral to weak alkaline	Acidic to neutral
	Fluid composition	Ca^{2+}–Mg^{2+}–Na^{+}–Cl^{-}–HCO_3^{-}–SO_4^{2-}–type, high Ca^{2+}/Mg^{2+} and CO_2, low Na^{+}/K^{+} and CH_4	Rich in K^{+}, Ca^{2+}, Cl^{-}, CH_4, $K^{+} > Ca^{2+} > Na^{+} > Mg^{2+}$, $Cl^{-} > F^{-}$
	Inclusion type	In addition to pure liquid-, gas - liquid phase inclusions, pure gas phase, containing crystal multiphase-, containing CO_2 polyphase inclusions	Pure liquid-, gas - liquid inclusions
	Complex	$[PbCl_4]^{2-}$and $[ZnCl_4]^{2-}$	Mainly chlorine complex, with secondary sulphur complex
	$\delta^{34}S_{CDT}$	+5‰~+15‰, strata sulphur is main origin	−39‰~+34.4‰, seawater sulphate is given priority for single origin or multiple sources
	$\delta^{13}C_{PDB}$	Dissolved carbon of marine carbonate is main source: 25.4‰~+7.7‰	Dissolved carbon of marine carbonate: 9.2‰~+0.1‰
	δD -$\delta^{18}O_{SMOW}$	Mixed fluid of deep-origin and basin fluids	Mainly atmospheric precipitation
	$(^{87}Sr/^{86}Sr)_0$	Mixed strontium occurs in ores; initial value is 0.7114, and mainly comes from the basement rock and deep sources	Initial value is 0.7074–0.7083
	Lead isotope of ore	Multiple sources; main source is crustal	Main source is upper crust
Ore-forming regularity	Ore-forming regularities	Hierarchical ore-controlling system of strike-slip fault-fold structures, facies of association mineralized alteration, typical mineralizing structure, zoning of mineral combination, and alteration, and metallogenetic geochemical barrier	Graben type tectonic belt of foreland basin, facies association of dissolved breccia collapsed in the unconformity surface, metallogenic normal fault fracture zone, calcium silicon - surface of regional activity of hot brine
	Ore-forming depth	≥1.5–2.5 km	≤1 km
	Ore-forming processes	Formation of oblique strike-slip structures and extensive fluid flow, injection of fluid into fault zones and differentiation of gas–liquid, and unloading of ore-forming fluid and coupled mineralization of structures and fluid	Karst formation of diagenetic carbonate, ore-forming fluid migration and filling

(Continued on following page)

TABLE 4 (*Continued*) Comparison of Zn–Pb deposits in the SYGT and typical MVT-type deposits.

Deposit types		Huize-style deposits	Typical MVT-type deposits
	Ore-forming model	Fluid 'injecting' and replacement	Hot brine in basin pump suction
Typical deposits		Huize, Maoping, Lehong, Zhugongtang, Qingshan, Tianbaoshan, and other Zn–Pb deposits in the SYGT	Huayuan, Limei, Dongjiahe, and other deposits in SW Hunan, Shiding, Beishan among others; deposits in Guangxi-Guangdong, Talmud Karan Pb–Zn deposit

Maping Fms. (C_2mp; upper Carboniferous), argillaceous sandstone, carbonaceous shale and inferior coal of the Liangshan Fms. (P_2l; Middle Permian), and marlite of the Yangxin Fms. (P_2y; Middle Permian). Among them, the crystalline limestone of the Maping formation is the main host rock of the deposit. The main fold structure is the Weining–Shuicheng anticline, which is a tight long axis fold with a NW-trending axis. There are two main groups of NW- and NE-trending faults; north–south trending faults are rare (Figure 1A). Hercynian diabase dikes are also exposed in the mining area, which has only a spatial relationship with Pb–Zn mineralisation.

The deposit is mainly composed of the No. 13, 14, and 15 rich Pb-Zn ore bodies, and the average grade of Pb and Zn is >30%. Among them, the No. 13 ore-body is 20–70 m long, with an average thickness of 32.10 m, and a dip extension depth of ~145 m; the average thickness of the No. 14 ore-body is 2.6 m, and the extension depth is >40 m; the length of the No. 15 ore-body is 42 m, the average thickness is 6.28 m, and the extension depth is >15 m. The ore-bodies are mainly distributed in the interlayer fault zone at the footwall of the F1 and F2 faults with a steep NW dip (Figure 7B). The strike of the ore-bodies is NW at 47°–70° with a SW dip, and is flanked by SE. The extension direction of the main ore-body is roughly the same as that of the NW-trending ore-hosting strata. The main ore-body appears in the form of sacs, blocks, breccias, and veins. The ore is mainly composed of galena, sphalerite, pyrite, calcite, barite, and a small amount of dolomite. They have euhedral subhedral and metasomatic residual structures and massive, stellar, breccia, disseminated, veinlet, and banded structures. The wall rock alteration is weak, only pyritisation, calcitisation, and baritisation are found. From the ore-body to the crystalline limestone, the mineral assemblage zoning of sphalerite + galena → pyrite + calcite is presented in turn. To date, the Pb-Zn metal reserves of the deposit are estimated to be> 300,000 tonnes. In recent years, stratoid rich and thick ore-bodies have been found on the side of F2 fault. Ore bodies are also found at 1,500 m depth in drilling holes within the Laoyingyan ore block, with a Pb-Zn grade of >30%. It is speculated that the deposit extends over a larger scale than currently recognised.

4 Ore-forming geochemistry of SYGT deposits

4.1 Fluid-inclusion geochemistry

The homogeneous temperatures and salinities of the mineral fluid inclusions in typical MVT deposits are approximately 90°C–150°C and 10–30 wt% NaCl eq., respectively (Basuki and Spooner, 2002; Leach et al., 2005). In contrast, the homogeneous temperatures of fluid inclusions from deposits in the SYGT are significantly higher. Higher ore-forming temperatures and medium salinities have been reported in the Huize and Maoping districts. Under conditions of no pressure correction, calcite fluid-inclusion data indicate that ore fluids had homogenisation temperatures of 183°C–223°C, with salinities reaching 13–18 wt% NaCl eq. However, brown sphalerite fluid-inclusion data, obtained *via* infrared micro-thermometry, show homogenisation temperatures of 250°C–355°C (without pressure correction) for salinities of ~1.8–4.0 wt% NaCl eq. (Han et al., 2007a; Han et al., 2016).

The fluid-inclusion types of two liquid-vapour phases (L_{H2O} +V_{H2O}) and a pure liquid phase (L_{H2O}) are similar to those from the MVT fluids (Huang et al., 2019a). Besides, there is also a pure vapour phase (V_{H2O}), three phases with a seed crystal (S + L_{H2O} +V_{H2O}), a CO_2-containing immiscible (V_{CO2} + L_{CO2} + L_{H2O}) fluid phase, and gas components that include CO_2, CH_4, and N_2 in the deposits throughout the SYGT area (Han et al., 2004; Han et al., 2007a). These characteristics differ from those of the MVT Zn–Pb deposits, showing that the immiscible processes and boiling of ore-forming fluids are the important ore-forming mechanisms in the mineralisation process for the Zn–Pb deposits in the SYGT (Figures 8A,B).

4.2 Isotope geochemistry

The sulphur isotope composition $\delta^{34}S_{CDT}$ values range from +5‰ to ~+15‰ for the deposits in the SYGT, which indicates that the sulphur originates from the strata, whereas $\delta^{34}S_{CDT}$ values in most MVT deposits (−39‰ to −34‰) show that sulphate primarily originates from the ocean (Figure 9). The C–H–O isotopes are complicated and their compositions in the SYGT deposits differ from those in the MVT deposits (Figure 10). Hydrogen and oxygen isotopes can effectively identify the ore-forming fluid source (Huang et al., 2019b). Zhang et al. (2017a) identified the two different metallogenic fluids by C-H-O isotope: a high temperature, low salinity, and acidic Fluid A, which originates from deep-seated fluids and is enriched in lighter C - O-H isotopes (−3‰ < $\delta^{13}C$‰ < −4‰; 10‰ < $\delta^{18}O$‰ <17‰; −92‰ < δD‰ < −50‰), and a low temperature, high salinity Fluid B, which is a subsurface brine formed by atmospheric precipitation. Fluid B is characterized by heavier C–O–H isotopic compositions (−2‰ < $\delta^{13}C$‰ < 1‰; 2‰ < $\delta^{18}O$‰ < 24‰; −66‰ < δD‰ < −43‰) than Fluid A and cycles continuously within the strata. By combining analyses of Sr-Nd-Pb tracers, Han et al. (2004; Han et al., 2007b) stress that the ore-forming elements in the deposits mainly derive from the folded Mesoproterozoic basement. The metallogenic fluid is a mix of a deep-origin fluid and basin fluid (Zhang et al., 2017b). The isotopic statistical data indicate that the initial value of mixed Sr in the ores (i.e., $^{87}Sr/^{86}Sr$ = 0.7114) is a deep basement signature.

5 Discussion

5.1 Typical SYGT deposit characteristics

Based on comprehensive analyses of the SYGT, as presented in the previous sections, we can summarise the typical geological characteristics of the deposits with the following eight main points.

1) High grade (Rich): The average grade of the Zn–Pb ores in the deposits is high (mostly Pb + Zn ≥ 20%–35%, even reaching 50%), far exceeding the typical grade in MVT Zn–Pb deposits (normally ~3%–10%) (Leach et al., 2005).
2) Large scale of single ore body (Large): Reserves of certain single ore-bodies (e.g., No. 1, 6, 8, and 10 in the Huize district and group Noes. One and six in the Maoping district) themselves comprise large-scale deposits, with 0.5–0.98 Mt of Pb and Zn metal reserves, as well as a Pb + Zn grades of ~25%–35%.
3) Multiple co-associated components (Numerous): Besides being rich in Pb and Zn, there are also enriched associated metallic elements, such as Ge, Ag, Cd, Ga, and In, among which certain combined elements can themselves constitute single ore-bodies (Table 2). The contents of the dispersed elements change dramatically and appear as large deviations in the ore-bodies, highlighting the non-uniformity and multiple stages of the ore-forming processes in the deposits.
4) Great depth of ore body extension (Deep): Unlike the MVT deposits, these deposits extend over a relatively small range of areas, but at great depth. For example, the Qilinchang deposit in the Huize district only extend over an area of 0.5 km^2. However, for this single main ore-body, its extension along dip (>1,800 m) along ore-controlling compressive-sheer fault zones in NEYD, which is beneficial to ore fluid migration driven by structure, is far more than theextension along its trend (150–350 m), where its features are similar to those of fault-controlled vein-type deposits in the orogenic belt (Chen et al., 2007).
5) Alteration intensity (Strong): Hydrothermal alteration is widespread and stronger, particularly appearing as strong hydrothermal dolomitisation (Han et al., 2007b; Han et al., 2012b). Assemblage zoning of pyritisation, dolomitisation, and calcitisation is evident around the ore-bodies in the deposits (Figures 4, 5). Typical mineral assemblages and zoning patterns of mineralisation/alteration indicate the presence of a metallogenic acid–alkali geochemical barrier.
6) Obvious mineral assemblage zoning (Zoning): There is clear zoning in the mineral assemblages in the ore-controlling fault zone, particularly in the NEYD. From the footwall to the hanging wall of the ore-bodies, zoning varies from a deep colour sphalerite + quartz + ferro-dolomite to brown and rosiness sphalerite + galena + pyrite, to pyrite + calcite + dolomite, showing that there are ore-forming fluid differentiations in the mineral crystallisations (Zhang et al., 2020).
7) Higher mineralization temperature (Higher): The homogenisation temperatures of the calcite fluid inclusions range from 183°C to 221 °C, with salinities from 13 to 18 wt% NaCl eq., while the homogenisation temperatures of dark sphalerite and quartz fluid inclusions range from 200°C to 355°C, with salinities from 1.eight to four wt% NaCl eq. (Figure 8). In addition to the liquid-rich gas–liquid two-phase (L_{H2O}+ V_{H2O}) and pure liquid phase (L_{H2O}), these types of fluid inclusions also contain three phases with a crystal (S + L_{H2O}+ V_{H2O}), three phases with CO_2 (V_{CO2} + Lco_2 + L_{H2O}), and a pure gas phase (V_{H2O}) fluid-inclusion. The gas phase components contain CO_2 + CH_4 + N_2 (Han et al., 2007a; Han et al., 2016; Zhang et al., 2017a). The results show that gas–liquid differentiation occurs during the ore-forming process. The rare earth element (REE) distribution patterns of calcite from the mineralisation phase indicate a four-grouping effect; that is, gas is also differentiated from the liquid during the ore-forming process (Huang et al., 2004).

5.2 Mechanical and kinematics of ore-bearing faults in different districts control ore-body orientations

Ore deposits controlled by oblique strike-slip structural belts. The mechanical and kinematic characteristics of differently trending faults in the different district result in different ore-body locations and lateral orientations.

All NE-trending compression-shear ore-bearinging interlayer fractures distinctly show sinistral transpressional movement features in the NEYD, where ore-bodies occur in the upper plate of major ore-controlling faults in the structural belts (Han et al., 2012a; Han et al., 2015), and resulted ore bodies to bend sideways towards SW-trending direction.

NW-trending tension-shear ore-bearing faults distinctly show right-hand transpressional movement characteristics in the NWGD, where vein ore-bodies mainly occur in the Yadu–Mangdong fault belt (e.g., the Zhugongtang deposit). Certain ore-bodies occur in the lower plates of the Weining–Shuicheng major faults (e.g., the Shanshulin, Qingshan, and Tianqiao deposits), and resulted ore bodies to bend sideways towards SE-trending direction.

The NWW-near EW-trending primarily shear ore-controlling faults between the Xiaojiang north–south-trending deep fault and the Puduhe fault distinctly show left-hand shear movement characteristics in the SWSD, and resulted ore bodies to bend sideways towards E or SEE-trending direction. There is a close relationship between strike-slip faults and folds dragged by faults (Han et al., 2012b). These situations reflect identical characteristics within the NW–SE-trending compressing stress processes during the metallogenic period. In addition, all boundaries between the ore-bodies and wall rocks are distinct (Han et al., 2007b; Han et al., 2012a), showing that ore-forming fluids may have been injected into fractures, possibly resulting in the rapid precipitation of metal sulphide.

5.3 Zn–Pb supernormal enrichment mechanisms

Numerical simulations have shown that large amounts of Zn and Pb metal can migrate through a chlorine complex. Physical chemistry phase diagrams indicate a lower pH, higher solubility, and enhanced ability to transport metals (Zhang et al., 2020). Moreover, hydrolysis experiments (Zhang et al., 2019a) indicate that a pH of less than four is a favourable condition for transporting a large number of metals. Precipitation experiments show that an increase in the pH can promote the precipitation of Pb-Zn sulphides, boiling affects the formation of ores at certain high grades, and mixing effects yield precipitation and mineralisation. The fluid inclusions, temperature measurements (Table 3), and isotopic compositions reveal the mixing of two fluid types (Zhang et al., 2017b).

5.4 Metallogenic regularities and Huize-style Zn–Pb deposits

Combined with the ore-forming conditions, the metallogenic theory of the Huize-style deposits (Han et al., 2014), and experimental geochemical research (Zhang et al. 2019a-Zhang et al., 2019b), the major controlling factors of the Zn and Pb supernormal enrichment mechanisms include the physicochemical conditions (e.g., pH value) in the hydrothermal system, adequate ore sources, boiling and mixing effects, and a strong tectonic driving force. As Table 3 summarises the physicochemical conditions of the ore-forming fluid and ore deposition in the Huize and Maoping Zn–Pb deposits, we observe that the original fluids had medium and high temperatures under acidic conditions, such that Pb and Zn ions were able to migrate as chloride complexes [i.e $(PbCl_4)^{2-}$ and $(ZnCl_4)^{2-}$]. When fluids flowed past the carbonate rocks and temperatures dropped to ~200°C, the neutralisation reaction led to the precipitation of metal sulphide. In summary, large-sized and super-large-scale rich Zn–Pb deposits formed in these conditions, which are favourable for a metallogenic tectonic setting, abundant mineral resources and fluids, a strong driving force (in terms of the strike-slip structure, superior storage space, strong decompression boiling, and mixing), 'injection', and replacement of the mixing fluid.

Based on the above comparison with respect to the typical geological and geochemical characteristics of Zn–Pb deposits in the SYGT and typical MVT deposits (Table 4), the metallogenic regularities of the deposits can be described in terms of the three following ore-forming factors: i) a strike-slip structure ore-controlling system, ii) typical mineral assemblages, and iii) mineralisation alteration zoning and a metallogenic acid–alkali geochemical barrier. Table 4 indicates that these deposits differ from the MVT deposits in terms of the metallogenic geological bodies, ore-forming structures, ore-forming fluid features, and ore-forming regularities.

According to the classic theory, MVT-type Pb-Zn deposits mainly form in cratonic carbonate platform and continental extensional environments, and in weakly deformed and stable carbonate platforms controlled by normal faults (Leach and Sangster, 1993).

The essential characteristics of MVT-type Pb-Zn deposits are epigenetic mineralisation; ore-bearing diagenetic carbonates (reef-limestone assemblages); no genetic relationship with magmatic activity; mainly Pb-Zn sulphide compositions; locations in the peripheries of cratonic platforms, foreland basins, and rift basins; related to basin fluids, ore-controlling normal faults, fissures, and karst caves; and low-temperature and high-salinity fluids (Leach and Sangster, 1993; Leach et al., 2001). Although some scholars have classified epigenetic hydrothermal deposits un-magma under different ore-controlling tectonic settings as MVT type deposits (Leach and Song, 2019), classic MVT theory cannot explain the formation mechanism of the Ge-rich Pb-Zn deposits in the SYGT area

Deposits in the SYGT area are the result of multiple geological effects, including strike-slip fault-fold structure trapping, rich mineral fluids, superior ore storage, fluid immiscibility, and mixing processes. These deposits are, therefore, particular to this region (Table 4). Based on the following four factors, we propose a new Huize-style Pb-Zn deposit, which is different from the classic MVT deposit (Han et al., 2012a; Han et al., 2014). First, in the metallogenic tectonic settings of Pb-Zn deposits in the SYGT, the main ore-controlling factors, mineralised alteration zoning laws, lateral plunging law of ore-bodies, ore-forming physicochemical conditions, geochemical characteristics, metallogenic mechanisms, and prospecting methods are all different from classic MVT deposits, such as the Huayuan Pb-Zn deposit distributed in the SE side area of the Xuefengshan tectonic belt in southwestern Hunan. Second, and more importantly, the prospecting investigation methods, used with respect to the MVT deposits and to the Huize-style deposits are markedly different. Third, this type of deposit was first discovered in the Huize Pb-Zn mine of Yunnan province along the SW margin of the Yangtze Continental Block. From a mining perspective, this deposit has been well known since ancient times because of its unique mineralisation characteristics (Han et al., 2012b). Fourth, certain deposits globally also show identical ore-forming features and metallogenic structural settings to the Huize-style deposits; for example, the La Calamine Zn–Pb deposit (Coppola et al., 2008), Iran's rich Zn–Pb deposit, and a series of large–super large Zn–Pb deposits in the Sanjiang area of the Tethys metallogenic belt. For example, the eastern Dongmozazhua Zn–Pb deposit in the Sanjiang metallogenic belt along the NE edge of the Qinghai-Tibet plateau belongs to the orogenic-type Zn–Pb-Ag–Cu (Hou et al., 2008) and MVT-like Zn–Pb deposits (Liu, 2012). These deposits are similar to the Huize-style Zn–Pb deposits in terms of their continental collision and orogeny backgrounds, where they were controlled by an oblique-slip structure. This also reflects the universality of the Huize-style deposits internally and abroad.

Based on the typicality of the Huize Zn–Pb deposits and the universality of the metallogenic features of this deposit type across the SYGT (Han et al., 2004; Han et al. 2006; Han et al. 2007a; Han et al. 2012b), new Huize-style Zn–Pb deposits have been proposed as a style of epigenetic Zn–Pb deposit. This deposit is named for the Huize ore district, which has had a strong association with mining in both ancient and modern times (Han et al., 2006). These deposits in the SYGT area are dominated by hydrothermal metasomatism against an intracontinental strike-slip tectonic background. The deposits formed from metallogenic fluids with medium–high temperatures (≥200°C–350 °C), low–medium salinity, and a CO_2-rich gas phase or gas-liquid-phase. These deposits ascended and injected into the fracture zones, such that they are mainly hosted by hydrothermal metasomatic carbonates. The conceptual model of ore deposit genesis sees Han et al. (2022).

5.5 Classification of deposit type and its significance

The classification of Zn–Pb deposits has posed a significant problem for prospecting predictions (Han et al., 2012a; Ye et al., 2017). Although the characteristics of the Huize-style deposits are different from those of the typical MVT deposits in terms of their tectonic setting, main ore-controlling factors, ore structures, physical-chemical conditions, and metallogenic models, among other factors (Table 4), the Huize-style deposits are representative of a new Pb-Zn deposit type, which is not contradictory to MVT deposits. We suggest that Huize-style deposits and typical MVT deposits are members of carbonate-hosted epigenetic hydrothermal-type Zn–Pb deposits of a non-magmatic origin, and constitute two unit-deposit types of the overall CNHT Zn–Pb deposits. Numerous deposits are characterised as a transitional type between the two (e.g., the Fankou super-large Zn–Pb deposit in eastern Guangdong).

The authors believe that the classification of deposit types is not only of theoretical significance, but also of the most important significance in guiding the exploration practice and prospecting deployment. The prospecting methods associated with the Huize-style deposits are different from those of typical MVT Pb-Zn deposits. Tectonic ore-control exploration techniques dominate the prospecting exploration of Huize-style deposits, such as ore-field structural analysis (Wang et al., 2020), tectono-geochemical exploration (Han et al., 2015), tectonic-altered rock facies measurements (Han, 2017; Wang et al., 2019), tunnel gravity exploration (Han et al., 2020), and electromagnetic detection (Han et al., 2019a). However, combinations of strata and lithology, with certain exploration techniques, such as ore-bearing sedimentary facies analysis, basin structure analysis, and geochemical exploration, dominate explorations of classic MVT deposits.

6 Conclusion

1) The following seven main points with the typical geological characteristics of the deposits have been summarised: rich, large, numerous, deep, strong, zoning, higher, controlled by oblique strike-slip structure. Mechanical and kinematic characteristics of ore-bearing faults of oblique strike-slip structural belts in different districts control ore-body orientations.
2) The sulphur isotope composition $\delta^{34}S_{CDT}$ values range from +5‰ to ~+15‰ for the deposits in the SYGT. There are two different metallogenic fluids in SYGT, one is enriched in lighter C and O isotopes, another is characterized by heavier C–O–H isotopic compositions than former. Sr-Nd-Pb tracers the ore-forming elements mainly originated from the folded Mesoproterozoic basement, and the metallogenic fluid is a mix of a deep-origin fluid and basin fluid.
3) Carbonate-hosted Zn–Pb ore deposits in the SYGT differ from classical MVT deposits in various aspects, such as their geological background, main deposit characteristics, geochemical features of the ore-forming fluids, metallogenic tectonic dynamic setting, and prospecting exploration methods. Consequently, a distinct Huize-style deposit has been proposed.
4) The important aim of classification of deposit types is in guiding the exploration practice and prospecting arrangement. Huize-style deposits and typical MVT deposits constitute two unit-deposit types in the CNHT. We anticipate the discovery of a number of Huize-style deposits across the globe in the near future.

Data availability statement

The original contributions presented in the study are included in the article/supplementary material, further inquiries can be directed to the corresponding authors.

Author contributions

HR: geofield survey, conceptualization, formal analysis, constructive discussions; ZY: writing-original draft, review and editing; DT, ZX, and WF: resources; QW and WM: data collection.

Funding

This research was jointly supported by the National Natural Science Foundation of China (grant nos. 42172086, 41802089, 41572060, U1133602), Yunnan Major Scientific and Technological Projects (202202AG050014), the Ten Thousand Talent Program of Yunnan Province (grant number YNWR-QNBJ-2019-157), projects of the YM Lab (2011), the Innovation Team of the Yunnan Province and Kunming University of Science and Technology (2008 and 2012).

Conflict of interest

Authors DT and ZX were employed by the company Sichuan Huidong Daliang Mining Co., Ltd. Author WF was employed Yunnan Metallurgy Resources Exploration Co., Ltd.

The remaining authors declare that the research was conducted in the absence of any commercial or financial relationships that could be construed as a potential conflict of interest.

Publisher's note

References

Basuki, N. I., and Spooner, E. T. C. (2002). A review of fluid inclusion temperatures and salinities in Mississippi Valley-type Zn-Pb deposits: Identifying thresholds for metal transport. *Explor. Min. Geol.* 11 (1-4), 1–17. doi:10.2113/11.1-4.1

Bradley, D. C., and Leach, D. L. (2003). Tectonic controls of Mississippi Valley-type lead–zinc mineralization in orogenic forelands. *Miner. Deposita* 38 (6), 652–667. doi:10.1007/s00126-003-0355-2

Chen, S. J. (1984). A discussion on the sedimentary origin of Pb-Zn deposits in western Guizhou and northeastern yunnan. *Guizhou Geol.* 8 (3), 35–39.

Chen, X. M., Deng, J., Shen, C. H., and Lan, J. Z. (2000). Physical and geochemical characteristics of ore-forming fluid in Fankou superlarge lead-zinc deposit. *Earth Sci.* 25 (4), 438–453.

Chen, Y. J., Ni, P., Fan, H. R., Pirajno, F., Lai, Y., Su, W. C., et al. (2007). Diagnostic fluid inclusion of different types hydrothermal gold deposits. *Acta Petrol. Sin.* 23 (9), 2085–2108.

Chen, Y. Q., and Zeng, B. F. (1984). Geology characteristics and Genesis of huge strata-bound lead-zinc ore deposit of Fankou, Guangdong. *Acta Sedimentol. Sin.* 2 (3), 34–47.

Cong, B. L. (1988). *Formation and evolution of the Pan-Xi paleorift*. Beijing: Science.

Cong, Y., Chen, J. P., Dong, Q. J., and Hao, J. H. (2010). Characteristics of sulfide minerals in dongmozhazhua lead-zinc deposit, Qinghai province, and their genetic significance. *Geoscience* 24 (1), 42–51.

Coppola, V., Boni, M., Gilg, H. A., Balassone, G., and Dejonghe, L. (2008). The “calamine” nonsulfide Zn–Pb deposits of Belgium: Petrographical, mineralogical and geochemical characterization. *Ore Geol. Rev.* 33 (2), 187–210. doi:10.1016/j.oregeorev.2006.03.005

Dong, C. J., Zhang, H. T., and Zhang, B. C. (2010). Analysis of the metallogenesis of qingchengzi Pb-Zn ore deposit. *Geol. Explor.* 46 (1), 59–69.

Fang, W. X. (2014). Geotectonic evolution and the proterozoic iron oxide copper-gold deposits on the western margin of the Yangtze massif. *Geotect. Metallogenia* 38 (4), 733–757.

Feng, G. Y., Liu, S., Peng, J. T., Zhang, Z. W., Qi, H. W., Zhu, X. Q., et al. (2009). Characteristics of fluid inclusions from Tamu kalangu lead zinc metallogenic belt, Xinjiang. *J. Jilin Univ. Sci. Ed.* 39 (3), 406–414.

Gao, J. G., Liang, T., Peng, M. X., Li, Y. L., Wang, L., and Gao, X. L. (2007). Sulfur, carbon, hydrogen and oxygen isotope geochemistry of Caixiashan lead-zinc deposit, Xinjiang. *Geol. Prospect.* 43 (5), 57–60.

Gao, X. L. (2006). *Geological characteristics and genetic mechanism of Caixiashan lead zinc deposit*. Xinjiang: Master, Chang’an University.

Greentree, M. R., Li, Z. X., Li, X. H., and Wu, H. C. (2006). Late Mesoproterozoic to earliest Neoproterozoic basin record of the Sibao orogenesis in Western South China and relationship to the assembly of Rodinia. *Precambrian Res.* 151 (1–2), 79–100. doi:10.1016/j.precamres.2006.08.002

Gu, S. Y. (2007). Study on the sulfur isotopic compositions of lead -zinc deposits in northwestern Guizhou province. *J. Guizhou Univ. Technol. Nat. Sci. Ed.* 36 (1), 8–11.

Guo, F., Fan, W. M., Wang, Y. J., and Li, C. W. (2004). When did the emeishan mantle plume activity start? Geochronological and geochemical evidence from ultramafic-mafic dikes in southwestern China. *Int. Geol. Rev.* 46 (3), 226–234. doi:10.2747/0020-6814.46.3.226

Han, R. S. (2017). “A method for locating and predicting large scale altered lithofacies of hydrothermal deposits,” in *State intellectual property office* (China.

Han, R. S., Chen, J., Huang, Z. L., Ma, D. Y., Xue, C. D., Li, Y., et al. (2006). *Dynamics of tectonic ore-forming process and localization-prognosis of concealed orebodies: As exemplified by the huize surper-large Zn-Pb-(Ag-Ge) district, yunnan*. Beijing: Science Press.

Han, R. S., Chen, J., Li, Y., Ma, D. Y., Gao, D. R., and Zhao, D. S. (2001a). Tectono-geochemical features and orientation prognosis of concealed ores of Qinlinchang lead-zinc deposit in Huize, Yunnan. *Acta Mineral. Sin.* 21 (4), 667–673.

Han, R. S., Chen, J., Wang, F., Wang, X. K., and Li, Y. (2015). Analysis of metal–element association halos within fault zones for the exploration of concealed ore-bodies — a case study of the Qilinchang Zn–Pb–(Ag–Ge) deposit in the huize mine district, northeastern yunnan, China. *J. Geochem. Explor.* 159 (11), 62–78. doi:10.1016/j.gexplo.2015.08.006

Han, R. S., Hu, Y. Z., Wang, X. K., Hou, B. H., Huang, Z. L., Chen, J., et al. (2012a). Mineralization model of rich Ge-Ag-bearing Zn-Pb polymetallic deposit concentrated district in northeastern yunnan, China. *Acta Geol. Sin.* 86 (2), 280–293.

Han, R. S., Li, B., Ni, P., Qiu, W. L., Wang, X. D., and Wang, T. G. (2016). Infrared micro-thermometry of fluid inclusions in sphalerite and geological significance of the huize super-large Zn-Pb-(Ge-Ag) deposit, yunnan province. *J. Jilin Univ. Earth Sci. Ed.* 46 (1), 91–104.

Han, R. S., Li, W. Y., Cheng, R. H., Wang, F., and Zhang, Y. (2020). 3D high-precision tunnel gravity exploration theory and its application for concealed inclined high-density ore deposits. *J. Appl. Geophys.* 180:104119–104210, doi:10.1016/j.jappgeo.2020.104119

Han, R. S., Li, W. Y., and Li, W. Q. (2019b). “A vector method for determining the occurrence factors of the source body of strip IP anomaly field,” in *State intellectual property office* (China).

Han, R. S., Liu, C. Q., Carranza, J. M., Hou, B. H., Huang, Z. L., Wang, X. K., et al. (2012b). REE geochemistry of altered fault tectonites of Huize-type Zn-Pb-(Ge-Ag) deposit, Yunnan Province, China. *Geochem. Explor. Environ. Anal.* 12, 127–146.

Han, R. S., Liu, C. Q., Huang, Z. L., Chen, J., and Li, Y. (2001b). On the metallogenic model of the Huize rich Zn–Pb deposit of Yunnan. *Acta Mineral. Sin.* 21 (4), 674–680.

Han, R. S., Liu, C. Q., Huang, Z. L., Chen, J., Ma, D. Y., Lei, L., et al. (2007a). Geological features and origin of the huize carbonate-hosted Zn–Pb–(Ag) district, yunnan, south China. *Ore Geol. Rev.* 31 (1), 360–383. doi:10.1016/j.oregeorev.2006.03.003

Han, R. S., Liu, C. Q., Huang, Z. L., Ma, D. Y., Li, Y., Hu, B., et al. (2004). Fluid inclusions of calcite and sources of ore-forming fluids in the huize Zn-Pb-(Ag-Ge) district, yunnan, China. *Acta Geol. Sin.* 78 (2), 583–591. doi:10.1111/j.1755-6724.2004.tb00170.x

Han, R. S., Wang, F., Hu, Y. Z., Wang, X. K., Ren, T., Qiu, W. L., et al. (2014). Metallogenic tectonic dynamics and chronology constrains on the huize-typ (HZT) germanium-rich silver-zinc-lead deposits. *Geotect. Metallogenia* 38 (4), 758–771.

Han, R. S., Wu, P., Zhang, Y., Huang, Z. L., Wang, F., Jin, Z. G., et al. (2022). New research progress in metallogenic theory for rich Zn-Pb(Ag-Ge) deposits in the Sichuan-Yunnan-Guizhou Triangle (SYGT) area, southwestern Tethys. *Acta Geol. Sin.*, 96(2):554–573.

Han, R. S., Zhang, Y., Wang, F., Wu, P., Qiu, W. L., and Li, W. Y. (2019a). *The metallogenic mechanism and localization-prognosis of concealed orebodies in rich Zn-Pb-(Ge) deposits at northeastern yunnan deposit concentration district, SW China*. Science Press.

Han, R. S., Zou, H. J., Hu, B., Hu, Y. Z., and Xue, C. D. (2007b). Features of fluid inclusions and sources of ore-forming fluid in the maoping carbonate-hosted Zn-Pb-(Ag-Ge) deposit, yunnan, China. *Acta Petrol. Sin.* 23 (09), 2109–2118.

Han, Y., Wang, J. B., Zhu, X. Y., Guo, N. N., Shun-Ting, L. I., and Wang, Y. L. (2011b). Geochemical charateristics of carbon and oxygen isotope in the Fankou lead-zinc Deposit,Guangdong and its geological impolications. *Geol. Explor.* 47 (4):642–648.

Hossini-Dinani, H., and Mohammad, Yazdi. (2021). Multi-dataset analysis to assess mineral potential of MVT-type zinc-lead deposits in Malayer-Isfahan metallogenic belt, Iran. *J. Arabaian Geosciences* 14 (673), 1–23.

Hou, Z. Q., Song, Y. C., Li, Z., Wang, Z. L., Yang, Z. M., Yang, Z. S., et al. (2008). Thrust-controlled, sediments-hosted Pb-Zn-Ag-Cu deposits in eastern and northern margins of Tibetan orogenic belt: Geological features and tectonic model. *Mineral. Deposits* (02), 123–144.

Huang, C. W., Du, G. F., Jiang, H. J., Xie, J. F., Zha, D. H., Li, H., et al. (2019a). Ore-forming fluids characteristics and metallogenesis of the anjing hitam Pb-Zn deposit in northern sumatra, Indonesia. *J. Earth Sci.* 30 (1), 131–141. doi:10.1007/s12583-019-0859-z

Huang, C. W., Li, H., and Lai, C. K. (2019b). Genesis of the binh do Pb-Zn deposit in northern vietnam: Evidence from H-O-S-Pb isotope geochemistry. *J. Earth Sci.* 30 (4), 679–688. doi:10.1007/s12583-019-0872-2

Huang, Z. L., Chen, J., and Han, R. S. (2004). *Geochemistry and ore gen-esis of huize super-large lead-zinc deposit, yunnan province, concurrently discuss the relationship between emeishan basalt and lead-zinc deposits*. Beijing, China: Geological Publishing House.

Kuang, W. L., Liu, J. S., Zhu, Z. Q., and Liu, S. H. (2002). Probe into kalangu MVTType lead-zinc deposit’s minerogenetic process and the source of minerogenetic material in west of kunlun. *World Geol.* (4), 28–34.

Kuang, W. L., Liu, J. S., Zhu, Z. Q., and Liu, S. H. (2003b). Study on the metallogenic mechanism of MVT type lead zinc deposit in Southwest Tarim-Taking kalanguu lead zinc deposit as an example. *Xinjiang Geol.* 21 (1), 136–140.

Kuang, W. L. (2003a). *The study on metallogenic geological conditions in west Kunlun mountain region and the metallogenic model of the Mississippi Valley type Pb-Zn deposit*. Ph.D, Central South University.

Leach, D. L., Bradley, D. C., Huston, D., Pisarevsky, S. A., Taylor, R. D., and Gardoll, S. J. (2010). Sediment-hosted lead-zinc deposits in earth history. *Econ. Geol.* 105 (3), 593–625. doi:10.2113/gsecongeo.105.3.593

Leach, D. L., Bradley, D., Lewchuk, M. T., Symons, D. T., Marsily, G. D., and Brannon, J. (2001). Mississippi Valley-Type lead–zinc deposits through geological time: Implications from recent age-dating research. *Miner. Deposita* 36 (8), 711–740. doi:10.1007/s001260100208

Leach, D. L., Sangster, D. F., Kelley, K. D., Large, R. R., Garven, G., Allen, C. R., et al. (2005). Sediment-hosted lead-zinc deposits: A global perspective. *Econ. Geol.* 100, 561–607.

Leach, D. L., and Sangster, D. F. (1993). *Mississippi Valley-Type lead-zinc deposits*, 40. Geological Association of Canada Special Paper, 289–314.

Leach, D. L., and Song, Y. C. (2019). *Sediment-hosted zinc-lead and copper deposits in China*. Society of Economic Geologists, Inc. SEG Special Publications, 325–409.

Li, Z. D. (2011). *Study on two main type of the lead-zinc deposits in sedimentary environment basin, southwestern Tianshan*, Xinjiang. Ph.D., China University of Geoscience(Beijing).

Li, Z. D., Xue, C. J., Zhang, S., Shi, H. G., and Wang, S. C. (2010). Geology,geochemistry and Genesis of huoshibulake Zn-Pb deposit in southwestern Tianshan,Xinjiang. *Mineral. Deposits* 29 (6), 983–998.

Liao, W. (1984). The features of S and Pb isotope and the discussion on model of metallogenic in Eastern of Yunnan and Western of Guizhou. *Geol. Depos.* (01), 2–6.

Lin, S. B. (1998). Geologic characteristic of Fankou super large-scale lead-zinc deposit. *Nonferrous Met.* S1, 3–12.

Liu, H. C., and Lin, W. D. (1999). *Metallogenic rules of Zn-Pb-(Ag) deposits in northeastern yunnan*. Kunming, China: Yunnan University Publishing House.

Liu, W. J., and Zheng, R. c. (2000). Characteristics and movement of ore-forming fluids in the Huayuan lead-zinc deposit. *Mineral. Deposits* 19 (2), 173–181.

Liu, Y. C. (2012). *Characteristics and metallogenic genesis of the carbon-ate-hosted lea-zinc deposits in the middle part of Sanjiang area, Ti-betan plateau*. Doctor, Chinese Academy of Geological Sciences.

Luo, J. L. (1995). Formation characteristics of super large deposits in Yunnan Province. *Yunnan Geol.* 14 (4), 276–280.

Luo, J. x. (2003). Characteristics of ore-controlling structure and Genesis of dongping lead-zinc deposit. *Yunnan Geol.* (3), 304–312.

Luo, Y. N. (1985). "Panzhihua-Xichang ancient rift zone in China," in *The proceedings of the Panzhihua-Xichang rift zone in China(1)*. Editor Yunxiang Zhang (Beijing: Geology Publishing House).

Ma, L., Chen, H. J., Gan, K. W., Xu, K. D., Xu, X. S., Wu, G. Y., et al. (2004). *Geology of marine oil and gas and tectonic in southern China*. Beijing: Geology Publishing House.

Mao, J. Q., Zhang, Q. H., and Gu, S. Y. (1997). The geological characteristics and tectonic evolution of Shuicheng fault subsidence. *J. Guizhou Univ. Technol.* (2), 4–9.

Peng, S. J. (1990). The geological charaeteristic and origin of major lead-zinc ore deposits in Kas-gar region Xinjiang nonferrous metals. 2:8–16.

Qiu, L., Yan, D. P., Tang, S. L., Wang, Q., Yang, W. X., Tang, X., et al. (2016). Mesozoic geology of southwestern China: Indosinian foreland overthrusting and subsequent deformation. *J. Asian Earth Sci.* 122, 91–105. doi:10.1016/j.jseaes.2016.03.006

Rui, Z. Y., Li, N., and Wang, L. S. (1991a). *Basin brine ore-forming and lead isotope targets of Guanmenshan lead-zinc deposit*. Beijing: Geology Publishing House.

Rui, Z. Y., Li, N., and Wang, L. S. (1991b). *Geothermal brine mineralization and lead isotope targeting in Guanmenshan lead zinc deposit basin*. Beijing: Geological Press.

Shen, S. (1988). *The metallogenic rule ore-search orientation of the major ore resources at the Xichang–Middle Yunnan area*. Chongqing: Chongqing Publishing House.

Song, X. Y., Hou, Z. Q., Cao, Z. M., Lou, J. R., Wang, Y. L., Zhang, C. J., et al. (2001). Petrogeochemical characteristics and time limit of large Basaltic igneous province. *Acta Geol. Sin.* 75 (4), 498–506.

Tang, Y. Y., Xianwu, B. I., Liping, H. E., Liyan, W. U., Feng, C. X., and Zou, Z. C. (2011). Geochemical characteristics of trace elements,fluid inclusions and carbon-oxygen isotopes of calcites in the Jinding Zn-Pb deposit,Lanping,China. *Acta Petrol. Sin.* 27 (9), 2635–2645.

Tao, Y., Ma, Y. S., Miao, L. C., and Zhu, F. L. (2009). SHRIMP U-Pb zircon age of the Jinbaoshan ultramafic intrusion, Yunnan Province, SW China. *Chin. Sci. Bull.* 54 (1), 168–172. doi:10.1007/s11434-008-0488-x

Tu, G. C. (1984). *I vols*. Beijing: Science Press.Geochemistry of strata-bound ore deposits in China.

Tu, G. C. (1987). *Geochemistry of strata-bound ore deposits in China. II vols*. Beijing: Science Press.

Tu, G. C. (1989). *III vols*. Beijing: Science Press.Geochemistry of strata-bound ore deposits in China.

Wang, L., Jiang, Z., Han, R., Tian, X., Li, Y., Zhu, E., et al. (2019). The first discovery of super-large-sized Rb deposit in changchengling mining area of southern hunan China. *J. Kunming Univ. Sci. Technol. (Nat. Sci.* 44 (4), 1–4).

Wang, M. Z., Han, R. S., and Zhang, Y. (2020). The control effect of metallotectonic system on lead-zinc metallogenic system: A case study of the huize deposit, yunnan province. *Acta Geol. Sin.* 94 (10), 3008–3023.

Wang, Q. (2008). *Enrichment regularity and mechanism of dispersed elements Cd, Ge and Ga of typical lead-zinc deposits in the eastern edge of Kangdian Axis*. Ph.D. , Chengdu University of Science and Technology.

Wang, S. L., Wang, D. B., Zhu, X. Y., Wang, J. B., and Peng, S. L. (2002). Ore-fluid geochemistry of tamu-kala Pb-Zn deposit in xinjiang. *Geology-geochemistry* 30 (4), 34–39.

Wang, X. C. (1991). Genesis anlysis of Daliangzi Pb-Zn deposit in sichuan province. *Mineral Resour. Geol.* 3, 151–156.

Wen, C. Q., Cai, J. M., Liu, W. Z., Qin, G. J., and Cheng, S. F. (1995). Geochemical charateristics of fliud inclusions in the Jinding lead-zinc deposit, Yunnan, China. *J. Mineralogy Petrology* (4), 78–84.

Xia, X. J., and Shu, J. W. (1995). The geological features and Genesis of Limei Pb-Zn deposit. *Geotect. Metallogenia* (3), 197–204.

Xiao, Q., Qin, K., Xu, Y., San, J., Ma, Z., Sun, H., et al. (2009). A discussion on geological characteristics of Hongxingshan Pb-Zn(Ag) deposit in Middle Tianshan massi, eastern Xinjiang, with reference to regional metallogenesis. *Mineral. Deposits* 28 (2), 120–132.

Xu, X. H., Long, X. R., Wen, C. Q., and Liu, W. Z. (1996). Study on the source of ore-forming material of the Chipu lead-zinc ore deposit, Sichuan. *J. Mineralogy Petrology* (3), 54–59.

Xue, C. J., Chi, G. X., Chen, Y. C., Zeng, R., Gao, Y. B., and Qing, H. R. (2007). The fluid dynamic process of large-scale mineralization in the lanping basin, yunnan, SW China: Evidence from fluid inclusions and basin fluid modeling. *Earth Sci. Front.* 14 (5), 147–155. doi:10.1016/s1872-5791(07)60042-6

Yan, D. P., Qiu, L., Wells, M. L., Zhou, M. F., Meng, X., Lu, S., et al. (2018). Structural and geochronological constraints on the early mesozoic north longmen Shan thrust belt: Foreland fold-thrust propagation of the SW qinling orogenic belt, northeastern Tibetan plateau. *Tectonics* 37 (12), 4595–4624. doi:10.1029/2018tc004986

Yang, S. X., and Lao, K. T. (2007). A tentative discussion on Genesis of lead-zinc deposits in northwest Hunan. *Mineral. Deposits* 26 (3), 330–340.

Yang, X. R., Peng, J. T., and Ruizhong, H. U. (2010). Sulfur isotopes characteristics and Genesis of Tamu lead and zinc ore deposit,southwest margin of Tarim,Xinjiang. *Acta Petrol. Sin.* 26 (10), 3074–3084.

Ye, T. Z., Wei, C. S., Wang, Y. W., Zhu, X. Y., and Pang, Z. S. (2017). *Theory and method of prospecting predictions in exploration area (monograph)*, VI-VII. Beijing: Geological House.

Yin, H. H., Yu, C. M., Zhang, G. X., and Lu, J. L. (1983). Sedimentaryand reformed Pb-Zn deposits in China. *Chin. Sci. (Part B)* 11, 1029–1038.

Yuan, H. H., Liu, M. D., and Zhang, S. F. (1985a). "Isotopic geochronology of magmatic rocks in the Panxi paleorift," in *Contributions to the panzhihua-xichang rift*. Editor Yunxiang Zhang (Beijing: Geological Press House), No.1.

Yuan, H. H., Zhang, S. F., Zhang, P., Liu, D., Shi, Z. M., Shen, F. K., et al. (1985b). "Isotopic geochronology of the magmatic rocks in the Panxi paleorift," in *Corpus of the Panxi paleorift studies in China*. Editor Z. YX (Beijing: Geological Publishing House), 241–257.

Zhai, Y. S., Yao, S. Z., and Cai, K. Q. (2011). *Mineral deposits*. Beijing: Geology Publishing House.

Zhang, W. J. (1984). A preliminary discussion on the sedimentary origin and metallogenic rule of Pb-Zn deposits in Northeastern Yunnan. *Geol. Explor.* 7, 11–16.

Zhang, X. C. (1989). Geological characteristics and chemical composition of deep ores in the No.1 ore-body of the Kuangshanchang Zn–Pb deposit—A research report

Zhang, Y., Han, R. S., Ding, X., He, J. J., and Wang, Y. R. (2019a). An experimental study on metal precipitation driven by fluid mixing: Implications for Genesis of carbonate-hosted lead–zinc ore deposits. *Acta Geochim.* 38 (2), 202–215. doi:10.1007/s11631-019-00314-4

Zhang, Y., Han, R. S., Ding, X., Wang, Y. R., and Wei, P. T. (2019b). Experimental study on fluid migration mechanism related to Pb–Zn super-enrichment: Implications to mineralisation mechanisms of the Pb–Zn deposits in the Sichuan–Yunnan–Guizhou, SW China. *Ore Geol. Rev.* 114 (103110), 1–19.

Zhang, Y., Han, R. S., and Wei, P. T. (2020). *The order of sphalerite and galena precipitation: A case study from lead-zinc deposits in southwest China*, 27. Journal of Central South University, 288–310.

Zhang, Y., Han, R. S., Wei, P., and Wang, L. (2017a). Identification of two types of metallogenic fluids in the ultra-large huize Pb–Zn deposit, SW China. *Geofluids*. 2017: 1–22, doi:10.1155/2017/6345810

Zhang, Y., Han, R., Wei, P., and Qiu, W. (2017b). Fluid inclusion features and physicochemical conditions of the Kuangshanchang Pb-Zn Deposit,Huize,Yunnan province. *J. Jilin Univ.* 47 (3), 719–733.

Zhang, Y. X., and Yuan, X. C. (1988). *Panxi Rift*. Beijing: Geological Publishing House.

Zhang, Z. Y. (2003). An analysis of geology and Genesis of Lehong Pb-Zn deposit. *Yunnan Geol.* 22 (1), 97–106.

Zhao, Z. (1995). Metallogenic model of Zn–Pb deposits in northeastern Yunnan. *J. Yunnan Geol.* 14 (4), 350–354.

Zhen, Q. G. (1997). Convection–circulating metallogenesis of the Kuangshanchang and Qilinchang Zn–Pb deposits at Huize and hydrothermal solution-derived massive Zn–Pb-rich ore-bodies-practice and understanding. *Mineral Resour. Geol. Southwest China* 11 (1–2), 8–16.

Zheng, H. F., Guo, F. S., Zhu, Z. J., and Jiang, Y. B. (2012). Carbon,oxygen and sulfur isotope geochemistry characteristics of the Jinding lead-zinc deposit in Yunnan and their geological significance. *Resour. Surv. Environ.* 33 (4), 218–224.

Zhong, H., and Zhu, W. G. (2006). Geochronology of layered mafic intrusions from the Pan–Xi area in the Emeishan large igneous province, SW China. *Miner. Deposita* 41 (6), 599–606. doi:10.1007/s00126-006-0081-7

Zhong, S. J., and Mucci, A. (1995). Partitioning of rare Earth elements (REEs) between calcite and seawater solutions at 25°C and 1 atm, and high dissolved REE concentrations. *Geochimica Cosmochimica Acta* 59 (3), 443–453. doi:10.1016/0016-7037(94)00381-u

Zhou, C., Wei, C., Guo, J., and Li, C. (2001). The source of metals in the Qilinchang Zn-Pb deposit, northeastern yunnan, China: Pb-Sr isotope constraints. *Econ. Geol.* 96 (3), 583–598. doi:10.2113/gsecongeo.96.3.583

Zhou, C. X. (1996). *Metallogenetic mechanism of qilingchang Pb-Zn deposit, northeastern yunnan province, China*. Ph.D., The Institute of Geochemistry, Chinese Academy of Sciences.The source of mineralizing metals, geochemical characterization of ore forming solution.

Zhou, M. F., Malpas, J., Song, X. Y., Robinson, P. T., Sun, M., Kennedy, A. K., et al. (2002). A temporal link between the Emeishan large igneous province (SW China) and the end-Guadalupian mass extinction. *Earth Planet. Sci. Lett.* 196 (3), 113–122. doi:10.1016/s0012-821x(01)00608-2

Zhou, M. F., Zhao, J. H., Qi, L., Su, W. C., and Hu, R. Z. (2006). Zircon U-Pb geochronology and elemental and Sr–Nd isotope geochemistry of Permian mafic rocks in the Funing area, SW China. *Contributions Mineralogy Petrology* 151 (1), 1–19. doi:10.1007/s00410-005-0030-y

Zhou, Z. D., Wang, R. M., and Zhuang, R. L. (1983). *The Gensis of Huayuan-Yutang lead-zinc deposit, Hunan Province*, 3. Journal of Chengdu University of Technology, 1–19.

Zhu, H. P., and Zhang, D. Q. (2004). Research on geology & geochemistry of silurian clastic rock - bearing lead-zinc deposit in southern Qinling. *Discuss. Geol. Prospect.* 19 (2), 76–82.

Zhu, X., Wang, J., Liu, Z., and Fang, T. (2010). Geologie characteristics and the Genesis of the Wulagen lead-zinc deposit, Xinjiang, China. *Acta Geol. Sin.* 84 (5), 694–702.

Zhu, X. Y., Wang, D. B., and Wang, S. L. (1998). *Geology and sulfur isotope geochemistry of the Tamu-Kalangu lead-zinc deposits.* Akto County, Xinjiang: Mineral Deposits, 204–214.3.

Zhu, X. Y., Wang, J. B., Liu, S. B., Wang, Y. L., Han, Y., and Zhen, S. M. (2013). Metallogenica age of Mississippi Valley Type Pb-Zn deposit in Fankou, Guangdong: Evidence from SHRIMP U-Pb zircon dating of diabase. *Acta Geol. Sin.* 87 (2), 167–177.